2010

Impact Of Hurricanes On Structures - A Performance Based Engineering View

Vijay Mishra
University of Central Florida

IMPACT OF HURRICANES ON STRUCTURES – A PERFORMANCE BASED ENGINEERING VIEW

by

VIJAY KUMAR MISHRA

B.E. Shri G.S. Institute of Science and Technology, 2006

A thesis submitted in partial fulfillment of the requirements
for the degree of Masters in Civil Engineering
in the Department of Civil, Environmental & Construction Engineering
in the College of Engineering and Computer Sciences
at the University of Central Florida
in Orlando, Florida

Spring Term

2010

ABSTRACT

The magnitude of damage caused to the United States (US) coast due to hurricanes has increased significantly in the last decade. During the period 2004-2005, the US experienced seven of the costliest hurricanes in the country's history (NWS TPC-5, 2007) leading to an estimated loss of ~ $158 billion. The present method for predicting hurricane losses, HAZUS (HAZard US), is solely based on hurricane hazard and damage caused to building envelopes only and not to structural systems (Vickery et al., 2006). This method does not take into account an intermediate step that allows for better damage estimates, which is structural response to the hazards that in turn can be mapped to the damage. The focus of this study was to quantify the uncertainty in response of structures to the hurricane hazards associated with hurricanes from performance based engineering perspective.

The study enumerates hazards associated with hurricanes events. The hazards considered can be quantified using a variety of measures, such as wind speed intensities, wave and surge heights. These hazards are quantified in terms of structural loads and are then applied to a structural system. Following that, structural analysis was performed to estimate the response from the structural system for given loads. All the possible responses are measured and they are fitted with suitable probability distribution to estimate the probability of a response. The response measured then can be used to understand the performance of a given structure under the various hurricane loads. Dynamic vs. static analysis was performed and results were compared. This will answer a few questions like, if there is any need to do both static and dynamic analysis and how hurricane loads affect the structural material models.

This being an exploratory study, available resources, research, and models were used. For generation of annual or extreme values of hazard, various available wind speed, storm surge, and

wave height models were studied and evaluated. The wind field model by Batts et al. (1980) was selected for generation of annual wind speed data. For calculation of maximum storm surge height, the Sea, Lake Overland Surges from Hurricane (SLOSH, Jelesnianski et al., 1992) program was used. Wave data was acquired from a National Oceanic and Atmospheric Administration (NOAA) database. The (extreme or annual) wind speed, surge height, and wave height generated were then fitted by suitable probability distributions to find the realizations of hazards and their probabilities. The distribution properties were calculated, correlations between the data were established, and a joint probability distribution function (PDF) of the parameters (wind speed, wave height, and storm surge) was generated.

Once the joint distribution of extreme loads was established, the next step was to measure the dynamic response of the structural system to these hazards. To measure the structural response, a finite element model of three-story concrete frame were constructed. Time histories of wind load were generated from wind net pressure coefficients recorded in a wind tunnel test (Main and Fritz, 2006). Wave load time histories were generated using laboratory basin test (Hawke's et al., 1993) wave height time history data and were converted into wave loads using Bernoulli's equation. Surge height was treated as a hydrostatic load in this analysis. These load time histories were then applied to the finite element model and response was measured. Response of the structural system was measured in terms of the mean and maximum displacements recorded at specific nodes of model. Response was calculated for loads having constant mean wind speed and surge/wave and different time histories.

The dominant frequency in the wind load time histories was closer to the natural frequency of the structural model used than the dominant frequency in the wave height time histories. Trends in the response for various combinations of mean wind speed, wave height, and

surge heights were analyzed. It was observed that responses are amplified with increase in the mean wind speed. Less response was measured for change in mean surge/wave height as the tributary area for wave forces was less compared to wind force. No increase in dynamic amplification factor was observed for increase in force time histories case.

ACKNOWLEDGEMENT

Special thanks to Dr. Kevin Mackie for all of his support and guidance throughout this thesis project. I would also like to thank Dr. Necati Catbas and Dr. Manoj Chopra for serving on my committee and providing great feedback for improving the thesis manuscript. Thanks to my parents and friends for all their love and support. Special thanks to my fiancé Neera, for being with me during this difficult time and giving me encouragement to perform and supported me in writing this thesis.

TABLE OF CONTENTS

LIST OF FIGURES x

LISTS OF TABLES xiv

LIST OF ABBREVIATIONS xv

CHAPTER ONE: INTRODUCTION 18

CHAPTER TWO: LITERATURE REVIEW 21

Hurricane Associated Hazards 21

1. Maximum Wind Speed 21
2. Storm Surge Height 24
3. Wave Height 24
4. Scour 25
5. Hurricane Flooding 27
6. Wind/Water Borne Debris and Other Secondary Hazards 27

Performance-Based Engineering 29

Performance Based Earthquake Engineering 29

Performance-Based Hurricane Engineering 31

Data Assisted Design (wind time history analysis) 31

Wind Field model 31

Storm Surge Model 32

Open System for Earthquake Engineering Simulation (OpenSEES) 33

CHAPTER THREE: METHODOLOGY 35
Research Structures & Location 35
Finite Element Model 37
Identifying Hazards 38
Quantifying Hazards 38
Probability Distribution Analysis 40
Spectral Analysis 41
Generating Data 43
Wind Speed Data 43
Storm Surge Data 45
Wave Height data 47
Load Calculation 49
Loads Cases 50
Structural Analysis 50
CHAPTER FOUR: RESULTS 52
Probability Distribution Analysis 52
Spectral Analysis 55
Structural Analysis 60
Response Probability Analysis 77
CHAPTER FIVE CONCLUSION 79

CHAPTER SIX FUTURE STUDIES AND RECOMMENDATIONS..... 83

APPENDIX ADDITIONAL RESULTS AND PLOTS..... 84

REFERENCES 93

LIST OF FIGURES

Figure 1 Cross section of hurricane structure with eye of hurricane at center (Holmes, 2001) ... 22

Figure 2 Recorded maximum wind speed near Miami Dade during hurricane Andrew 1992 (Jelesnianski, 2005) ... 23

Figure 3 Recorded storm surge near Miami Dade during hurricane Andrew, 1992 (Jelesnianski, 2005) ... 23

Figure 4 Scour occurring below Ground floor during hurricane Katrina (NIST-1476, 2006) ... 26

Figure 5 Windborne debris puncturing concrete wall (Holmes, 2001) ... 26

Figure 6 Performance Based Methodology Chart Developed by Pacific Earthquake Engineering Research (PEER) ... 30

Figure 7 Three story three bay concrete frame model created in OpenSEES ... 37

Figure 8 Hazards Quantification Methodology in this study ... 39

Figure 9 Histogram of 1000 year simulated maximum non-directional wind speed at 10 meter above ground over open terrain ... 41

Figure 10 Time history of displacement recorded at node 52 in FEM model for nonlinear dynamic analysis case NL1200805 ... 42

Figure 11 Power spectrum of displacement time history recorded at node 52 in FEM model for nonlinear dynamic analysis case NL1200805 ... 42

Figure 12. 1000 year simulated 1-minute wind speed data at 10m above ground Miami-Dade (Batts, 1985) ... 44

Figure 13 Wind tunnel pitched roof model with Pressure tab location on the pitched roof glass model (Main and Fritz 2006) ... 45

Figure 14 Grid model from SLOSH representing Miami- Dade (Jelesnianski, 1992) ... 46

Figure 15 Histogram of 25-year Significant Wave height generated at Virginia Key, Fl (NOAA) 48
Figure 16 CDF of 1000 year simulated maximum non-directional wind speed data 52
Figure 17 CDF of Cat-3 Storm Surge 53
Figure 18 Joint probability plot for Mean wind speed and surge height 54
Figure 19. Joint probability plot for mean wind speed and wave height 55
Figure 20 Power spectrum of recorded wind speed data at edge column 56
Figure 21 Variation of auto and cross correlation with time lag of 0.045sec on windward side . 57
Figure 22 Variation of auto and cross correlation with time lag of 0.045sec on windward and leeward side 57
Figure 23 Wave spectra for wave generated from simulation and laboratory test using input wave height 0.12m and peak period 1.8 seconds 59
Figure 24 Wave spectra for wave generated laboratory test at CHL using input wave height 0.12m and peak period 1.8 seconds 59
Figure 25 Variation of auto and cross correlation of wave data with time lag of 0.75sec for lab test C and D 60
Figure 26 Moment Curvature at the bottom of column for three directional coordinates of building on windward side 61
Figure 27 Total base Shear Vs Displacement at node 52 in X direction 62
Figure 28 Nonlinear Dynamic response Vs linear static response case NL0800805 64
Figure 29 Nonlinear Dynamic response Vs linear static response case NL16000805 65
Figure 30 Dynamic amplification factor for load case NL0800805 65
Figure 31 Dynamic amplification factor for load case NL1600805 66

Figure 32 Displacement trend for variable mean wind speeds and constant surge and wave height 67
Figure 33 Base shear Vs Displacement for load case LN0800805 67
Figure 34 Base shear Vs Displacement for load case NL0800805 68
Figure 35 Base shear Vs Displacement for load case LN1600805 68
Figure 36 Base shear Vs Displacement for load case NL1600805 69
Figure 37 Power spectrum of linear material model response for variable wind speed and constant surge and wave height 70
Figure 38 Power spectrum of nonlinear material model response for variable wind speed and constant surge and wave height 71
Figure 39 Power spectrum of linear and nonlinear material model response for constant wind speed and surge and wave height 71
Figure 40 Displacement trend for variable mean surge height and constant wind speed and wave height 73
Figure 41 Power spectrum of linear material model response for variable mean surge height and constant mean wins speed and wave height 73
Figure 42 Power spectrum of nonlinear material model response for variable surge height and constant mean wind and wave height 74
Figure 43 Power spectrum of linear and nonlinear material model for constant mean wind speed, surge height, and wave height 74
Figure 44 Displacement trend for variable wave height and constant wind speed and surge height 75

Figure 45 Power spectrum of linear material model response for variable wave height and constant mean wind speed and surge height 75
Figure 46 Power spectrum of nonlinear material model response for variable wave height and constant mean wind speed and surge height 76
Figure 47 Power spectrum of linear material model response for constant wave height, mean wind speed and surge height 76
Figure 48 Histogram of response probability analysis for additional 72 load cases. 78
Figure 49 Trends of maximum and mean response of linear and nonlinear model for Mean wind speed of 80 mph 85
Figure 50 Trends of maximum and mean response of linear and nonlinear model for Mean wind speed of 100 mph 85
Figure 51 Trends of maximum and mean response of linear and nonlinear model for Mean wind speed of 120 mph 86
Figure 52 Trends of maximum and mean response of linear and nonlinear model for Mean wind speed of 140 mph 86
Figure 53 Trends of maximum and mean response of linear and nonlinear model for Mean wind speed of 160 mph 87

LISTS OF TABLES

Table 1 Costliest United States Hurricanes, 1900-2006 (Blake et al. 2007) 19

Table 2 Statistics of global disaster from 1950 to 1999, adapted from Munich Re (1999) and Wang et al. (2000) 21

Table 3 Saffir-Simpson scale (NOAA, 2009) 28

Table 4 Basic Modeling Parameters of Structure 36

Table 5 Concrete material Properties (concrete02) 36

Table 6 Steel Material Properties (steel02) 36

Table 7 Load case used in the analysis 63

Table 8 Maximum and mean response of linear and nonlinear model for Mean wind speed of 80 mph 88

Table 9 Maximum and mean response of linear and nonlinear model for Mean wind speed of 120 mph 90

Table 10 Maximum and mean response of linear and nonlinear model for Mean wind speed of 140 mph 91

Table 11 Maximum and mean response of linear and nonlinear model for Mean wind speed of 160 mph 92

LIST OF ABBREVIATIONS

ΔP_{max}	Central pressure difference
ρ	Density of water,
A	Tributary area.
ADCIRC	ADvanced CIRculation model for oceanic, coastal and estuarine waters
ASCE	American Society of Civil Engineers
ATC	Applied technology council
C_p	Pressure coefficient
CDF	Cumulative Distribution Function
d	Water depth or surge level
DAD	Data Assisted Design
FEMA	Federal Emergency Management Agency
g	Acceleration due to gravity
H	Wave height,
HURDAT	HURricane DATabase
HAZUS	HAZard US

IAHR	International Association for Hydro environmental engineering and Research
k	Wave number,
LRFD	Load and Resistance Factor Design
NIST	National Institute of Standards and Technology
NOAA	National Oceanic and Atmospheric Administration
NWS	National Weather Service
PBE	Performance Based Engineering
PEER	Pacific Earthquake Engineering Research
PBEE	Performance Based Earthquake Engineering
SEAOC	Structural Engineering Association of California
SLOSH	Sea, Lake Overland Surges from Hurricane
SWH	Significant Wave Height
TCL	Tool Command Language
UWO	University of Westerns Ontario
WAM	Wave Analysis Model
R_{max}	Maximum hurricane radius
V_m	Mean wind speed representing category of hurricane

V_t	Translational wind speed
z	Variation in water level,

CHAPTER ONE:

INTRODUCTION

Tropical cyclones having a maximum wind speed greater than or equal to 74mph are termed hurricanes. Available data show that every year, hurricanes make a landfall along the Atlantic and Gulf of Mexico coastline of the United States. Out of the ten costliest natural disasters in the history of United States, six were caused by hurricanes (NWS TPC-5, 2007), Hurricane Katrina itself cost ~$84 billion (see Table 1 Costliest United States Hurricanes, 1900-2006 (Blake et al. 2007)worth of damage. The wind speed associated with hurricanes is not by itself the greatest cause of damage. However, when coupled with storm surge and flooding, the potential of damage is greatly amplified. The United States has been hit by 279 hurricanes along its coastlines between the years 1851-2006. Of the total, 96 were major hurricanes (NWS TPC-5, 2007), and every year the number keeps rising due to the changing environmental conditions.

In addition, according to a NOAA report (NWS TPC-5, 2007), it has been observed that the population has grown along the United States coastlines. Fifty million residents have moved to coastal area in past twenty-five years, consequently creating difficulties for emergency managers. The number of deaths due to hurricanes may have gone down with improved technology, emergency response, and modern infrastructure, but economic losses have increased significantly. Despite having state-of-the-art forecasting systems, it is still difficult to fully measure the impact of hurricanes. Almost every structure; major buildings, levees, floodwalls, bridges, railroads, airports, seaports, utilities, residential structures, etc., are affected by hurricanes. In reconnaissance reports after hurricane Katrina (NIST-TS-1476, pp180), experts commented that present codes and design methodologies were not able to predict the hazards and damage caused by hurricane Katrina. Hence there is need to revise the present design

methodology. The idea of performance-based engineering presented here could be one such solution to the above problem where by the direct and indirect losses of infrastructure due to hurricane event could be estimated with certain probability. This methodology might be able to fill the present gap between the hazards and losses during a hurricane event

Table 1 Costliest United States Hurricanes, 1900-2006 (Blake et al. 2007)

Rank	Hurricane	Category	States effected	Year of occurrence	Damage
1	Katrina	3	FL, LA, MS	2005	$81,000,000,000
2	Andrew	5	FL, LA	1992	$26,500,000,000
3	Wilma	3	FL	2005	$20,600,000,000
4	Charley	4	FL	2004	$15,000,000,000
5	Ivan	3	AL, FL	2004	$14,200,000,000

The objective of this study is to quantify the uncertain response of structures to the predominant hazards associated with hurricanes. A performance-based approach currently used in assessment of other hazards, particularly earthquakes, is used as a basis for conducting this study. In current codes of practice, load and resistance factor design (LRFD) and allowable stress design (ASD), structural components are designed in a manner that they are never exposed to the load that may cause it to fail. Whereas in performance-based design, all the possible responses are calculated for all the potential loads for a given design. These responses are then mapped to a damage level, which sequentially could to be mapped to losses. Hence, knowing the hazard, response, damage, and loss, a choice can be made based on acceptable losses that may be incurred or to redesign the structure. The drawback of performance-based engineering is that it needs multiple steps of design and analysis before achieving satisfactory level of losses. Hence,

structural designers are not willing to switch to PBD from LRFD/ASD as it may be more computational and time consuming. However, the integration of present computation technology and PBD has great possibilities in the future.

The performance-based methodology was developed in two parts in this study. In the first part, all the possible hazards associated with the hurricane were identified. The hurricane hazards causing maximum damage to structure, namely wind speed, surge height, and wave height, were then chosen. The marginal distributions defining each hazard were identified. These marginal distributions were then used to find the joint probability of the occurrence of hazards. In the second part, the three critical hurricane hazards identified above were then used to perform structural analysis. A three-story three-bay model of a concrete frame was created in OpenSEES and hazards were converted into loads before applying them to the structure for analysis. Four alternative methods of structural analysis, namely linear static, linear dynamic, nonlinear static, and nonlinear dynamic were performed. Linear static analysis was performed to create an envelope of possible response whereas nonlinear static analysis was performed to validate the model and identify probable failure locations. Depending upon the mean wind speed and wave/surge height, 250 load cases for dynamic analysis were created. Linear and nonlinear dynamic analyses were performed and responses were compared. It was found that for wind speed below category 3 the linear and nonlinear responses were almost equal. For higher wind speeds, nonlinear analysis gave higher response values than linear analysis.

CHAPTER TWO:

LITERATURE REVIEW

Earthquakes and hurricanes are two different kinds of extreme events. Hurricanes and earthquake have multiple hazards associated with them that impact the performance of structures. The most common hazards associated with earthquake are earthquake intensity, liquefaction, landslide, etc., whereas hazards associated hurricane are wind speed, surge height, wave height, and water/air borne debris. Prior to the analysis of hurricane loads on the structure, it is important to understand all the possible hazards associated with hurricane events.

Table 2 Statistics of global disaster from 1950 to 1999, adapted from Munich Re (1999) and Wang et al. (2000)

Disaster Type	**Earthquake**	**Hurricane**	**Flood**	**Others**	**Total**
Number of Occurrences	68	89	63	14	234
Casualties (million people)	0.66	0.63	0.1	0.01	1.4
Economic Losses (billion US$)	336	268.8	288	67.2	960
Insurance Losses (billion US$)	25.4	68.7	8.5	8.4	111

Hurricane Associated Hazards

1. Maximum Wind Speed

Hurricanes are tropical cyclones with a maximum wind speed of 74 mph or more. They occur in latitude 5° and above on both sides of the equator, and are most powerful between latitude 20° - 30°. The structure of the hurricane is shown below in Figure 1 Cross section of hurricane structure with eye of hurricane at center (Holmes, 2001). The meteorological parameters commonly used in defining hurricane are maximum wind speed (V_m), central pressure difference (ΔP), translational wind speed (V_t), storm direction (θ), and maximum wind

speed radius (R_{max}). Hurricanes consist of a circulating wind field with low pressure and slowest wind speed area known as the eye of hurricane in the center. As one moves away from center of eye, the wind speed increases and is maximum just outside the eye. The velocity of hurricane wind decreases as it go further away from eye and is slowest at end of hurricane radius, hurricane wind speed changes with height and are slowest near ground.

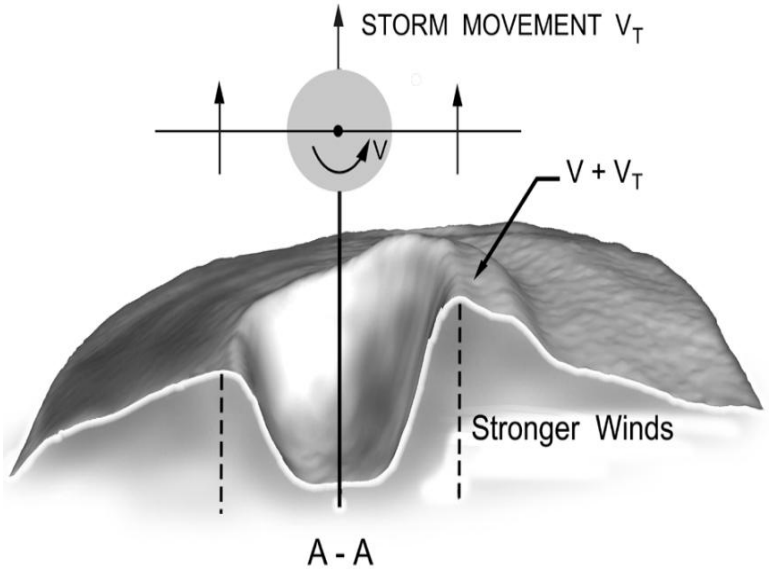

Figure 1 Cross section of hurricane structure with eye of hurricane at center (Holmes, 2001)

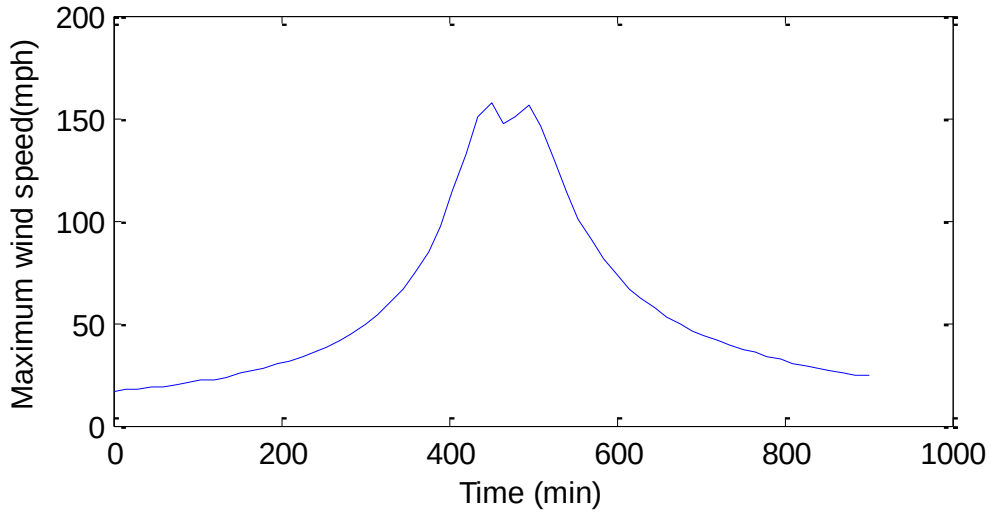

Figure 2 Recorded maximum wind speed near Miami Dade during hurricane Andrew 1992 (Jelesnianski, 2005)

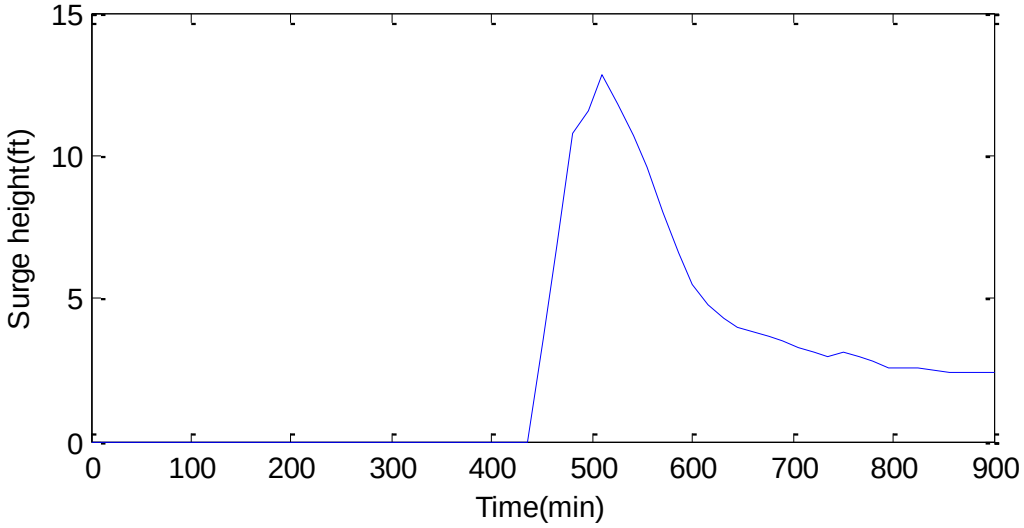

Figure 3 Recorded storm surge near Miami Dade during hurricane Andrew, 1992 (Jelesnianski, 2005)

2. Storm Surge Height

Storm surge is an unusual rising of water above the normal mean sea level due to an imminent hurricane near the coast Figure 3 Recorded storm surge near Miami Dade during hurricane Andrew, 1992. Surge height starts just before the hurricane making a landfall and is greatest when the storm center reaches the coast. Until the last quarter of last century, it was assumed that the surge heights were the product of high wind speeds, but recent hurricane events have forced researchers to think alternatively (Durham et al, 2007). Surge heights are caused by a combination of various astronomical conditions, meteorological condition, and topology of the oceanic basin. Meteorological parameters that affect the storm surge are the central pressure difference (ΔP), maximum wind speed (V_m) at the eye of storm, translational (forward) wind speed, and size of storm (R_{max}**).** Hurricanes have lower central pressures, but high pressures around the storm center. This pressure difference causes the rise of water at the storm center. This meteorological phenomenon is called the inverted barometer effect. When a storm circulates over the sea surface, it generates currents in the sea water. As soon as this storm makes a landfall, the currents generated by high-speed wind are impeded leading to the abnormal rise of water level.

The other key factor that causes storm surge rise is astronomical tides. A surge height is amplified when a hurricane makes a landfall during high tide and deamplified during low tide. Storm surge height also depends on the continental shelf slope. If the slope is steep, there is less chance that the surge height will reach an inland location and vice versa.

3. Wave Height

Wave height is the difference in elevation between adjacent crests and troughs of a sea wave. When the water surface is disturbed, it produces waves. These waves propagate further

due to the disturbance of adjacent water surfaces. This disturbance in the sea is caused by wind blowing over a vast stretch of sea surface. For the period of hurricane, the disturbance in sea is extremely high leading to increased surface oscillation consequently resulting into high storm waves. During hurricane Ivan, the wave height reached up to 27.7 m in the sea. When a hurricane makes landfall it leads to the breaking of hurricane waves on shore producing set-up and set-down waves. Wave set-ups and set-downs are the increase and decrease in water level in shallow water area (surf zones and coastal areas) due to transfer of energy of water momentum to water level due to wave breaking phenomenon. The sizes of set-up/set-down waves or infra-gravity waves are approximately 10-25% of incident significant waves. Hurricane induced storm surge and waves cause maximum damage to US coasts (Wu et al., 2003)

4. Scour

Once a hurricane has passed, scour is the primary reason for damage caused to bridge and building foundations. Two kinds of scour phenomena can occur, namely shear-induced scour and liquefaction-induced scour. Amongst them, the liquefaction-induced scour is more widespread during the hurricane event (Robertson et al, 2008). The liquefaction scour can be explained by the periodic formation of crest and trough of waves over the soil matrix. Subsequently, this leads to changes in pore pressure, causing disturbance of soil matrix resulting in flow of soil particles below the foundation. Eventually, this results in uneven settlement of structures. Liquefaction-induced scour is amplified by the fast drawdown of water in inundated area.

Figure 4 Scour occurring below Ground floor during hurricane Katrina (NIST-1476, 2006)

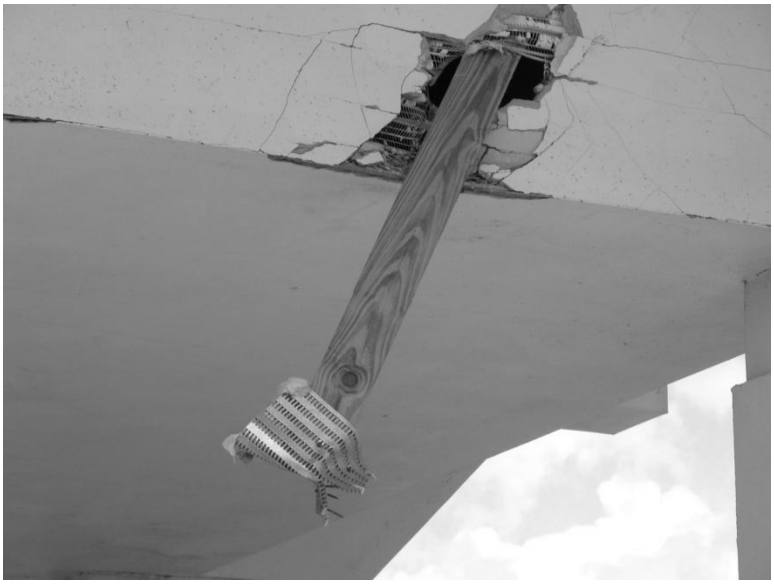

Figure 5 Windborne debris puncturing concrete wall (Holmes, 2001)

5. Hurricane Flooding

Flooding is the main reason for fatalities during hurricane events (NOAA/PA 20052, 2000). Two kinds of flooding occur during hurricane events. They are known as rainfall-induced flooding and surge-induced flooding. One or both can occur during hurricanes. Surge-induced flooding affects areas where a hurricane has made landfall, but rainfall-induced flooding can occur at the place of landfall as well as areas miles away from the landfall location. Rainfall-induced flooding is not directly related to the intensity of hurricane alone, rather it depends on other meteorological factors. The effect of flooding on structures during hurricanes is amplified due to other hazards like wave and surge as it elevate the mean water level.

6. Wind/Water Borne Debris and Other Secondary Hazards

Windborne debris is the primary cause behind the failure of the building envelope in low and high-rise structures (Holmes, 2001 and Vickery, 2006). Waterborne debris flowing at a speed may cause damage to columns and footings of structures. When flowing debris accumulate between columns or near foundations, it can lead to obstruction in the flow of water resulting in water damming. There are some secondary hazards associated with hurricanes that may also affect structures during hurricane. Some of the common secondary hazards include fire, landslide, and other environmental hazards.

Previous attempts have been made to quantify hurricane associated hazards, among them, the Saffir-Simpsons scale (see Table 3 Saffir-Simpson scale is most common and readily used. The Saffir-Simpson scale was formulated by Herbert Saffir, a consulting engineer, and Dr. Bob Simpson, director of the National Hurricane Center. This scale was developed for helping forecasters and disaster management experts to predict possible damage due to hurricane events.

However, this scale is largely subjective and is not useful for quantitative hazards for probabilistic analysis.

Table 3 Saffir-Simpson scale (NOAA, 2009)

Category	Wind speed	Storm surge	Example
Category I (weak)	< 95 mph	4-5 ft	Hurricane Lili (2002),
Category II (Moderate)	96-110 mph	6-8 ft	Hurricane Frances (2004),
Category III (Significant)	111-130 mph	9-12 ft	Hurricane Ivan (2004)
Category IV (severe)	131-155mph	13-18 ft	Hurricane Charley (2004)
Category V	> 155 mph	> 18 ft	Hurricane Andrew (1992)

Performance-Based Engineering

Performance-based engineering entails prediction of the structural response with a certain probability for a given structure under a given extreme loading condition. Prior to the development of performance-based earthquake engineering, the concept of performance-based engineering was already in use in the nuclear industry. Recent documents on PBE in the field of earthquake engineering include those from the Structural Engineering Association of California (SEAOC), Vision 2000 (Hamburger, 1995). As per SEAOC, PBEE is defined as a method for designing, maintaining, and constructing a building such that they are capable of providing predictable performance when affected by earthquake. The framework of PBE was later extended to various engineering research fields involving extreme loads like wind, fire, waves and blast loads (Whittaker et al 2005).

Performance Based Earthquake Engineering

The concept of PBE was employed in the field of earthquake engineering even before the development of PBEE (FEMA 273 (1996), SEAOC (1995), ATC-40 (1996)., etc). Almost all the past earthquake codes and designs were somehow using the theory of PBE (Krawinkler & Miranda, 2004). LRFD is the most common example of use of PBE in design codes. The difference between LRFD and PBEE is that LRFD considers only two levels of responses, safe and collapse, while in PBEE a whole spectrum of responses (like safe, partially safe, unsafe etc.) is developed. Some of the most recognized efforts to outline and standardize the concept PBE were Vision 2000 (SEAOC, 1995), FEMA 273 (1996), FEMA 274 (1997), ATC-40 (1996) and FEMA 356 (2000). All the methods follow the same theory, which is to define some performance objectives and quantify them with a level of performance and hazard (Krawinkler and Miranda, 2004).

Performance based methodology is a four-step process. The initial step is to identify the seismic hazard called *Hazard Analysis*. Next, given the hazard inputs, *Structural Analysis* is performed to determine various engineering demand parameters like drift velocity and acceleration. Thereafter, based on the structural responses to hazard, *Damage* caused is assessed. Finally, these damages are quantified as *Losses* measured in terms of death, dollar and downtime.

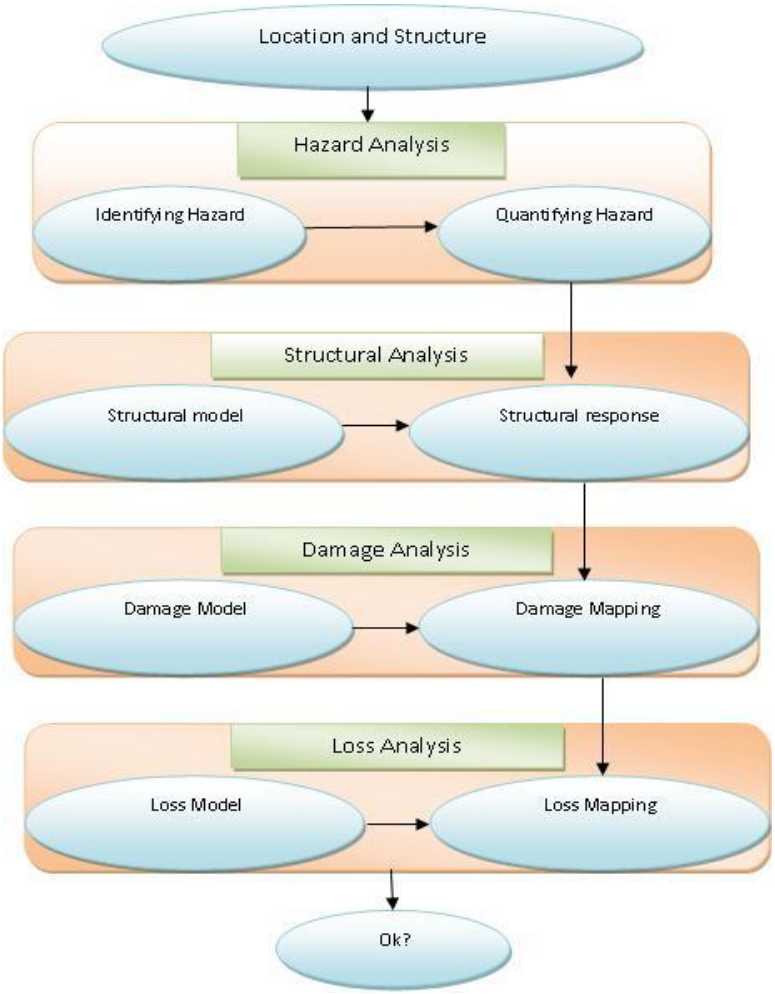

Figure 6 Performance Based Methodology Chart Developed by Pacific Earthquake Engineering Research (PEER)

Performance-Based Hurricane Engineering

Performance based hurricane engineering is a new method of analyzing structures subjected to hurricane hazards. There is little available research that looks at hurricane from performance-based perspective. This study will try to develop the idea during the course of this paper.

Data Assisted Design (wind time history analysis)

Data Assisted Design DAD presents a method in which a database of the directional pressure coefficient time history data is used directly for analysis and design of structural systems (Main and Fritz 2006). The database of the pressure tab for the analysis was developed in a series of wind tunnel tests (Ho et al., 2005). The data was generated using wind tunnel tests carried out at the boundary layer wind tunnel laboratory at UWO. This database was generated for two different terrain conditions, open and suburban with 1:100 scale models. The data in the wind tunnel was recorded at the frequency of 500 Hz for 100 seconds, which is equivalent to 22 Hz for 2304 seconds for full-scale open exposure. The structural model used in the test was a gable roof with variable eave heights. These time histories of pressure coefficient are used in the structural analysis in this study. To use them for structural analysis, the pressure coefficient time histories are multiplied by the square of mean wind speed (Main and Fritz, 2006). The mean wind speeds for the analysis were assumed 80, 100, 120, 140, and 160 mph representing each category of hurricane.

Wind Field model

Most of the early attempts in the field of engineering science to predict hurricane winds were based on probabilistic models. Batts et al. (1985) came up with the first mathematical model with probabilistic meteorological input. The Batts model consisted of two parts (1)

meteorological characters of hurricane and (2) mathematical model of hurricane wind. The meteorological characters included rate of occurrence, central pressure difference, translational wind speed, storm direction, maximum wind speed radius and crossing point coordinates. Batts mathematical model describes the relation between these meteorological characters to find surface wind speed using following relation.

$$V(z = 10, R) = 0.865V_{gx} + 0.5V_t$$

$$V_{gx} = K\sqrt{\Delta p_{max} - (\frac{Rf}{2})}$$

$$K = \left(\left(\frac{R * \alpha}{\rho}\right)\right)^{.5}$$

Where V_{gx} is maximum gradient wind speed, z = height above ground level, V = maximum wind speed, f = Coriolis parameter, R = radius of maximum wind, V_t = transitional wind speed, ρ = air density, α = parametric constant and Δp_{max} = central pressure difference. Batts generated 1000-year synthetic hurricane wind speed data using Monte Carlo simulation along the coast of the United States and Mexico. The statistical data input for Batts model came from HURricane DATabase (HURDAT, Jarvinen et al., 1984). Batts model was one of the preliminary models which was further improved by various others researchers like Georgious (1985), Neumann et al. (1991) and Vickery et al. (1995, 2000). The Vickery et al. (2000) procedure is the presently followed by ASCE 7-05 to produce design wind speeds.

Storm Surge Model

Several researchers have come up with different models for storm surge prediction. Some of the common surge models are Federal Emergency Management Agency (FEMA) surge model

by Tetra Tech Inc. (1984), SLOSH by the National Weather Service (NWS) and ADvanced CIRculation model for oceanic, coastal and estuarine waters (ADCIRC) by Luettich et al., (2002). ADCIRC is the most frequently used commercial storm surge model. The Sea, Lake Overland Surges from Hurricane (SLOSH) model is used in this study for generating storm surge data required for the analysis.

SLOSH has been developed as a model for emergency managers and local authorities to utilize in predicting maximum possible storm surge in specific basins. SLOSH is a numerical, dynamic, two-dimensional storm surge model developed by NWS. It is used for the real time forecasting of storm surge due to hurricanes in the Atlantic and Mexican coast of the US. Unlike Wind field model, SLOSH is a diagnosis model and not a predictive model. SLOSH divides the US coast into 41 basins and each basin is further divided into smaller curvilinear polar coordinate grids that allow for greater resolution within the basin. Basic transport equations of a water mass were developed by Platzman (1963) and modified by Jelesnianski (1967) and were used in SLOSH for calculation of storm surge.

Open System for Earthquake Engineering Simulation (OpenSEES)

OpenSEES is an open source finite element software developed by PEER at the University of California Berkeley for simulating response of structural and geotechnical component under earthquake loads. OpenSEES has a library of elements, solvers, and materials to perform almost any kind of structural and geotechnical analysis. OpenSEES does not have a user interface for input, rather it uses Tool Command Language (TCL) as the input format. OpenSEES also has an advanced tool to perform reliability analysis used in performance-based engineering. This program has been used in the field of earthquake as well as performance-based

engineering. OpenSEES was used as primary computation tool for dynamic analysis of the structure considered in this study.

CHAPTER THREE:

METHODOLOGY

As mentioned earlier, this study is an extension of performance-based engineering in the field of hurricane engineering. The methodology followed here is similar to that in Vision 2000. The process of PBHE is divided into four steps (1) *Hazard analysis* (2) *Structural Analysis* (3) *Damage Analysis* and (4) *Loss Analysis*. Hazard Analysis can be further sub divided into (a) identifying hazard and (b) quantifying hazard. Identifying hazard is a different process in performance based hurricane engineering compared to performance based earthquake engineering.

Research Structures & Location

An important aspect of performance-based analysis is that it is done for a specific structure and location. Miami-Dade in southern Florida has already faced many hurricanes and has a large amount of recorded hurricane data. Hence, it was chosen as location for this study. For this preliminary analysis, a generic structural model of three story three bay concrete frame is used as it represents most low-rise residential or office buildings. The height of each floor is 12 feet. Basic modeling parameters of the building are enumerated in Table 4 Basic Modeling Parameters of Structure, Table 5 Concrete material Properties (concrete02) and Table 6 Steel Material Properties (steel02). The floor and walls were not modeled in this analysis, but the floor weight was taken into consideration in this analysis.

Table 4 Basic Modeling Parameters of Structure

Property	Beam	Column	Girder
Width (inch)	6	12	6
Total length (feet)	60’	36’	60’
Depth (inch)	12	12	12
Total Reinforcement (in^2)	3.52	4.4	3.52
No of patch per section	10x10	10x10	10x10

Table 5 Concrete material Properties (concrete02)

Property	**Value**
Compressive Strength of Concrete (psi)	4000
Module of Elasticity of Concrete (ksi)	3604
Poisson’s ratio	0.2
Strain at Compressive strength	0.0022
Concrete crushing Strength (ksi)	0.8
Strain at crushing strength	.044
Ratio between unloading slope at crushing and initial slope	1
Concrete Tensile Strength (ksi)	.56

Table 6 Steel Material Properties (steel02)

Property	**Value**
Yield stress of steel (ksi)	66.8
Modules of Elasticity of steel (ksi)	29000
Strain Hardening ratio	0.01

Finite Element Model

Finite element model of three stories by three bay concrete frame was created in the OpenSEES for analysis. Mass is lumped at the nodes connected by two-node force beam-column elements. They were used to model the beam, columns and girder of the structure. Two different material models of concrete were used in the analysis. An elastic uniaxial material model of concrete was used in the linear dynamic analysis, whereas a nonlinear uniaxial material model was used for push over and nonlinear dynamic analysis. The bottom end of the first floor columns were assumed to be restrained for all six degrees of freedom. No floors or walls were modeled in the FEM, but the loads due to floors were added to the model. A damping ratio of 0.02 was applied in the model.

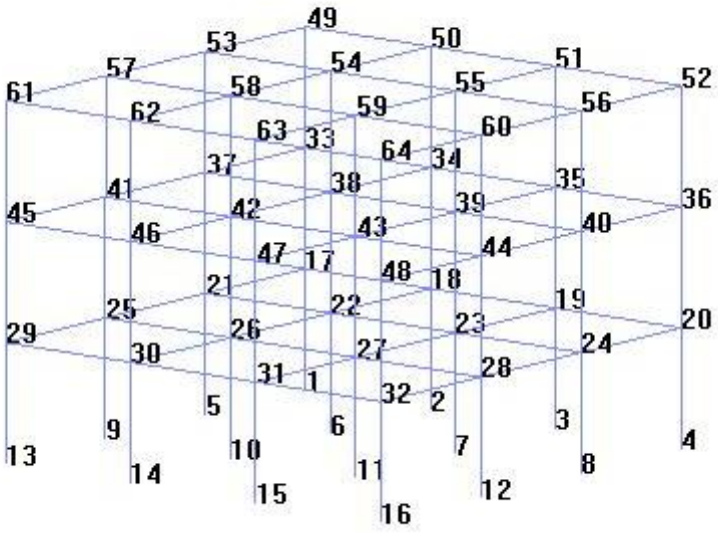

Figure 7 Three story three bay concrete frame model created in OpenSEES

Identifying Hazards

After conducting a sufficient amount of research, six primary and various secondary hazards were identified that were associated with the hurricane event. It was observed that out of these six hazards, storm surge with waves causes maximum damage to the structure. In the present study, three hazards (wind speed, storm surge and hurricane waves) are investigated further.

Quantifying Hazards

In the process of PBE, there are two parts of to every hazard analysis. The first part defines the general characteristics like mean wind speed, while the other is the uncertainty attached to the dynamic or time-variant characteristics, such as the turbulence in wind. In this study, two varieties of quantification were performed. Firstly, the annual data or mean data was quantified to perform probability distribution analysis. These probability distributions were then used to find a correlation between these hazards. This was followed by quantification of hourly data or time history data, which was used to carry out structural analysis. For these two types of quantification two different sets of data were required, namely the annual data and the hourly time histories. In order to create annual data, various meteorological models, simulation results and recorded data were used. While, in order to generate hourly time histories various recorded time histories were employed. The methods of generating and analyzing data are discussed below.

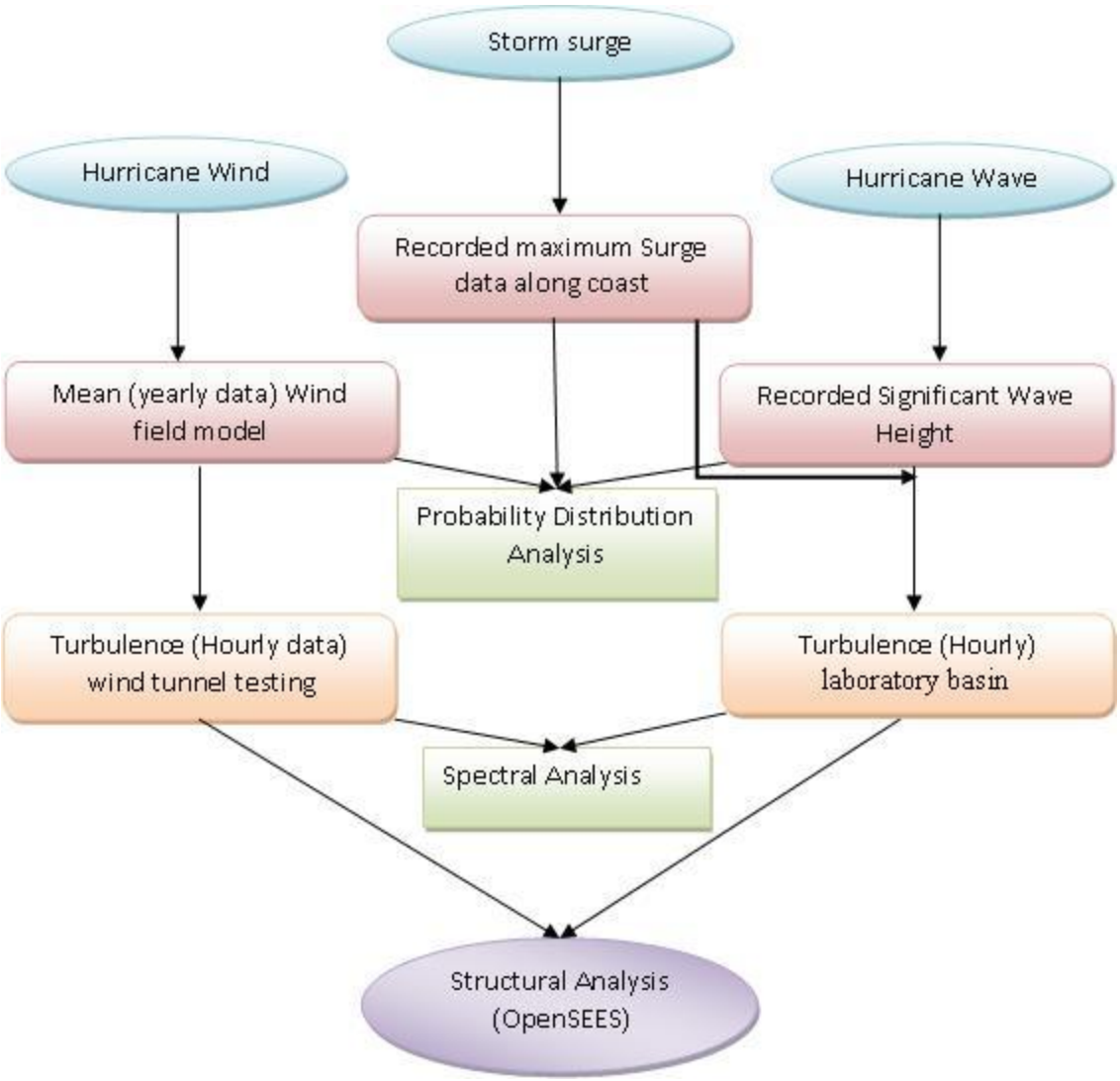

Figure 8 Hazards Quantification Methodology in this study

Probability Distribution Analysis

Hurricane wind is not the primary reason for structural damage, but they could be catastrophic when partnered with other hazards. Probability distribution analysis was carried out to find the magnitude and probability of occurrence of a hazard and its correlation with other hazards. To find the best probability distribution that can define hazard, a histogram of the annual and extreme recorded data was plotted. Subsequently, a curve was fitted to this histogram. Lastly, various existing distributions were compared with the fitted curve to find the most suitable probability distribution defining hazards for the given location. The process probability distribution analysis explained in following figures. First, the histogram of the 1000 year recorded data was plotted as shown in Figure 9, thereafter the histogram bars are fitted with curve using.

Once the marginal distributions defining the hazards are identified, the distribution properties of the marginal distribution are estimated. These distribution properties are then used for joint probability analysis. A joint probability distribution analysis was done to find the correlation between various hazards and how they act with each other. These joint probability distributions were then used to find the most suitable combination of load sets for the structural analysis. For example, if category 3 hurricane is going to make a landfall what are the possible surge and wave heights that can occur?

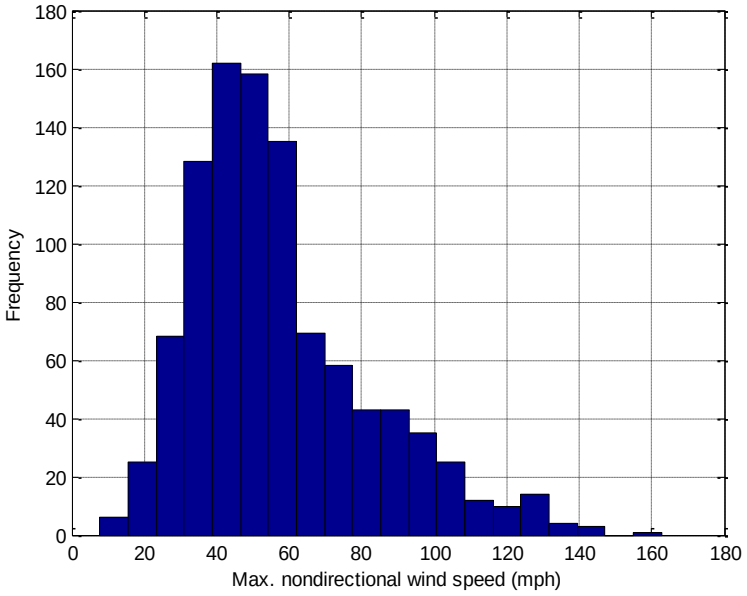

Figure 9 Histogram of 1000 year simulated maximum non-directional wind speed at 10 meter above ground over open terrain

Spectral Analysis

Spectral analysis was conducted to the find the prominent frequency in load time histories as shown in Figure 10 and Figure 11. These frequencies were then compared with the natural frequency of the structural system to find the possibility of resonance in structural system. The time histories of wind and wave are compared to earthquake time histories in terms of the prominent frequencies and their time periods. This comparison will help in understanding the response from structure with respect to earthquake Auto and Cross-correlation of the time histories were investigated to find the randomness in the time histories. Auto correlation function informs about the correlation between two data points in same time history. Whereas, the cross-

correlation coefficient defines the degree of correlation between two different time histories. The outcome of this analysis is discussed in the result section.

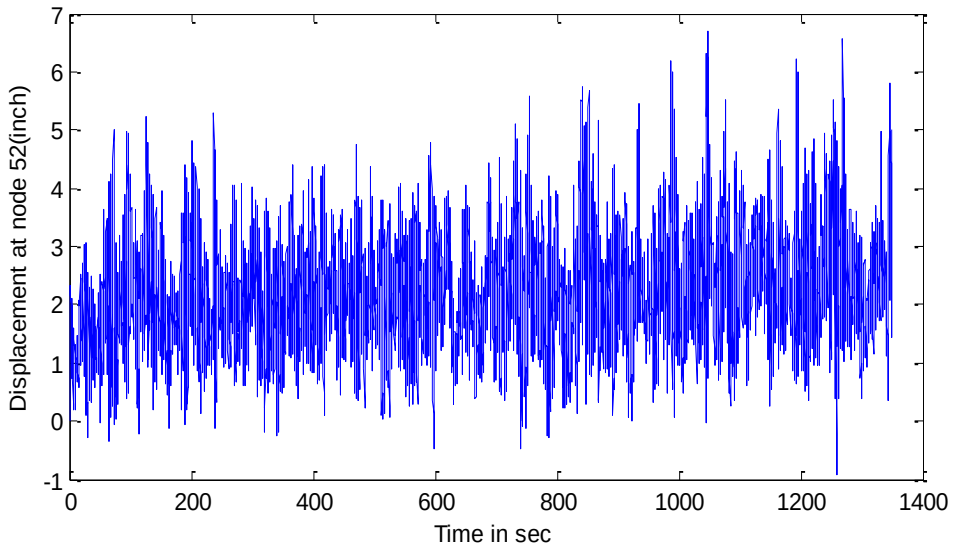

Figure 10 Time history of displacement recorded at node 52 in FEM model for nonlinear dynamic analysis case NL1200805

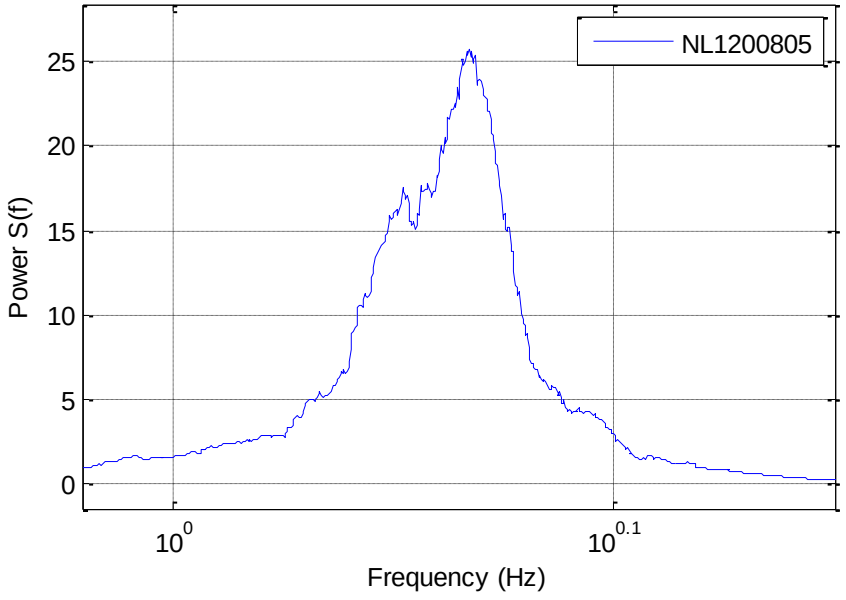

Figure 11 Power spectrum of displacement time history recorded at node 52 in FEM model for nonlinear dynamic analysis case NL1200805

Generating Data

Each hazard data used in this analysis were defined by two components. The first being the mean, which defines the general properties of the hazards and the second is the fluctuation superimposed on mean defining the uncertainty in hazards. Generation of the data was the most important and prolonged part of this study. Mainly due to this being, the exploratory study and unavailability of sufficient data source to be readily used. Various existing resources and studies were investigated for data collection. The process of data generation is discussed below

Wind Speed Data

Wind is a random and dynamic both in time and in space. This randomness in data can be defined by a mean and superimposed fluctuation on it. The mean factor is called mean wind speed. In this analysis, the mean data was created by methodology created by Batts et al. (1980). Batts performed the Monte Carlo simulation to generate 1000-year synthetic wind speed data for entire east coast of United States and Mexico (Figure 12). The results of Batts Monte Carlo simulation were extracted from NIST. The results of simulation included maximum wind speed at a mile marker for sixteen directions. The maximum of sixteen directions were recorded for probability distribution analysis. It is important to understand that the probability distribution of maximum wind speed will be different for different locations.

.

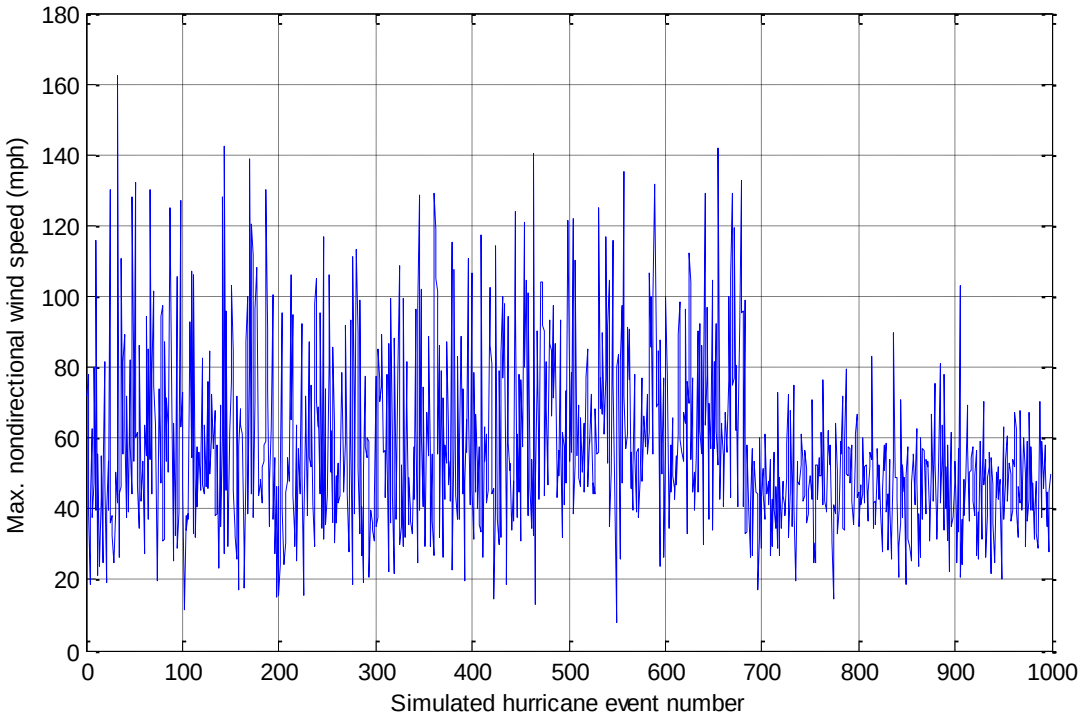

Figure 12. 1000 year simulated 1-minute wind speed data at 10m above ground Miami-Dade (Batts, 1985)

The randomness in mean wind was created by overlaying the mean with fluctuation created from recorded wind tunnel test time histories. These wind tunnel time histories were generated using NIST data source by Ho et al. (2005). The time histories created were in terms of net pressure coefficient on the surface and roof of gable roof structure. Three sets of time histories were generated based on the orientation of the building with respect to the wind tunnel axis. Before applying these time histories to the structure, pressure coefficients were converted into wind speed and Spectral Analysis was carried out. Results of the spectral Analysis were compared with Yu et al. (2008) and are discussed in the result section.

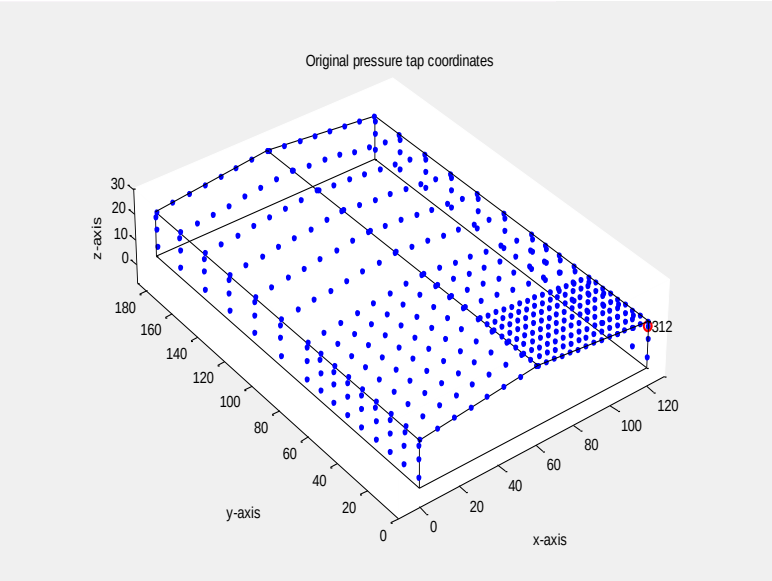

Figure 13 Wind tunnel pitched roof model with Pressure tab location on the pitched roof glass model (Main and Fritz 2006)

Storm Surge Data

Storm surge data for the analysis was generated from SLOSH. For this study, the Biscayne basin (near Dade County Miami) on the Atlantic coast of Florida was chosen. The SLOSH grid for Biscayne basin is shown in Figure 14 Grid model from SLOSH representing Miami- Dade. The Biscayne basin contains 162 curved lines and 88 radial lines making a grid mesh of 14256 regions.

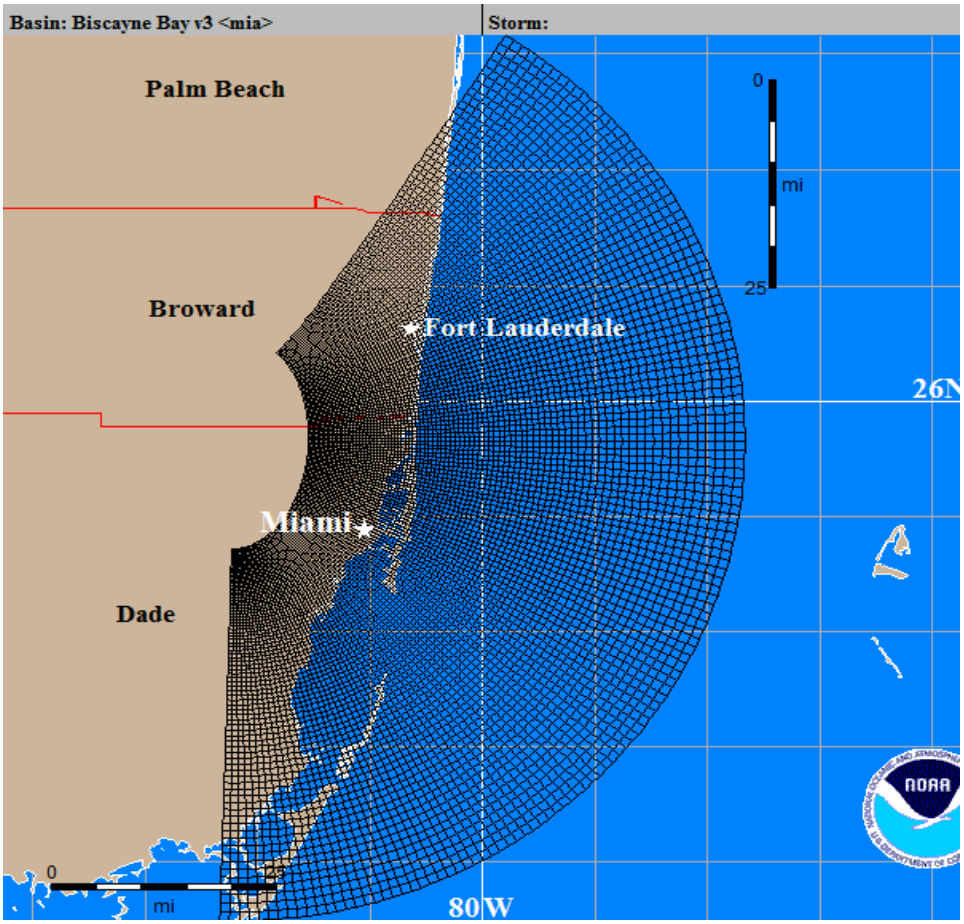

Figure 14 Grid model from SLOSH representing Miami- Dade (Jelesnianski, 1992)

The size of the grid increases with the distance from the pole, with an average size of the grid of approximately 0.3 square miles. This grid system provides greater resolution in the focus area because the surge value changes with the topography of the area. The user interface of the model has three inputs for calculation of storm surge. These inputs are (i) category of hurricane, (ii) direction of wind speed and (iii) forward wind speed with tide condition (high, medium and low). For the Biscayne basin, 32 regions along 21.1 miles of coast were earmarked and each region along the coastline was analyzed. The SLOSH results are usually in the form of maximum storm surge for a given category (1 to 5), direction (16 directions) and forward wind speed (5, 15, and 25 mph) for each region. However, for the purpose of this study direction was

disregarded and only storm surge for given category and forward wind speeds were recorded. The surge data were then fitted by a suitable distribution. The Gumbel distribution best fitted the surge data. Time histories for the surge were not generated, as they were treated as static load in the study.

Wave Height data

Similar to hurricane wind speeds, hurricane waves also consists of two components, namely Significant Wave Height (SWH) and wave fluctuation. SWH and fluctuating waves are comparable and similar to mean wind speed and turbulence in wind respectively. SWH is approximately equal to the average height of the highest of one- third of the waves during a sampling period. For generating SWH data, twenty-five years recorded NOAA's historical wave records for Virginia Key, FL were utilized. Thereafter SWH data was analyzed to fit suitable Probability distribution (Figure 15).

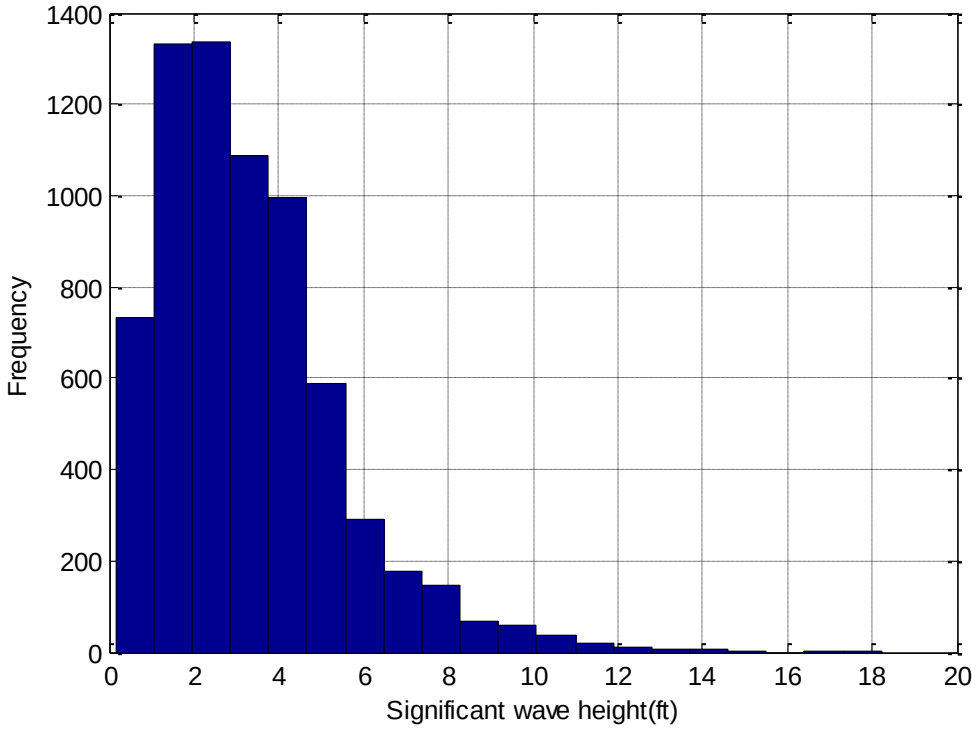

Figure 15 Histogram of 25-year Significant Wave height generated at Virginia Key, Fl (NOAA)

It is important to emphasis that during the event of a hurricane making a landfall, the set-ups and set-downs waves reach the inland structure and not the SWH. In this study, it has been assumed that the incident waves are the only source of setup waves. Hence, they have properties similar to the SWH.

For generating the fluctuation in the water level of set-up/set-down waves, the multidirectional wave data created by International Association for Hydro Environmental Engineering and Research (IAHR) were used. The test (A, B, C & D) was performed in laboratory basin at Canadian Hydraulic Center. The input wave for the test had significant wave height of 0.12 meter and peak period of 1.8 seconds. The outcome of the test was recorded in

terms of velocity and the wave height. The test ran for 1500 seconds at the sampling rate of 20 Hz, and the data was recorded at the middle of a pentagon shaped Moore. Spectral Analysis of the recorded time history was performed before applying them to the structure. Thereafter, recorded wave heights were magnified by the wave water level for dynamic structural analysis.

Load Calculation

Structural analysis was performed for five categories of hurricane. A mean wind speed representing each category of response was selected. In order to convert pressure coefficient time histories recorded from wind tunnel to force histories, they were scaled using equation (1).

$$F_{(WS)} = .5 * \rho_a * {V_m}^2 * C_p * A \quad \text{----------(1)}$$

Where ρ_a =.002377lbf.s^2/ft^4 at standard atmospheric condition, V_m= maximum wind speed, C_p = pressure coefficient and A= tributary area. Subsequently the tributary area was calculated from the plan of structure and node location at which the force time histories were applied.

To convert wave and storm surge into structural load Bernoulli equation for irrotational flow was used,

$$F_{(ww,ss)} = \left(\rho g z + .5\rho g H \left[\frac{\cosh\, k(d+z)}{\cosh\, kd}\right] \cos(kx - \sigma t)\right) A \quad \text{---------- (2)}$$

Where $F_{(ww,ss)}$= force due to hydrostatic surge and hydrodynamic wave loads, ρ = density of water, g = acceleration due to gravity, z = variation in water level, H = wave height, k= wave number h = surge level and $\cos(kx - \sigma t)$ is phase angle. In the abovementioned equation, the first term calculates the normal surge (hydrostatic) load while the second term computes the wave (dynamic) load due to wave induced particle acceleration. Since we were using the time histories, the phase angle was assumed as one. It was assumed that during hurricane the walls on

the first floor of the building would collapse. Hence, the tributary area for wave and surge load was the area of columns only. As there was no proper reference or source on how to apply load to an inland structure, it was assumed that the effective force on structure will be only 25% of calculated wave and surge force.

Loads Cases

Two loading scenarios were analyzed. In the first scenario, five realizations of each hazard were identified. For wind speed the realizations were 80, 100, 120, 140 and 160 mph whereas, for surge height the realizations were 2, 4, 6, 8 and 10 ft. Finally, the realizations for the wave height were 0.5, 1, 1.5, 2 and 2.5 ft. 125-load combinations of these hazard realizations were made and applied to structure for analysis. These 125 cases were applied to both linear and nonlinear material models resulting into total 250 load cases for parametric analysis. In the second scenario, different load time histories of same mean wind speed and wave /surge height were created. For a mean wind speed of 100mph, surge height of 4ft and maximum wave height of 1.5 ft 72 load cases were created for response probability analysis. Total of 322 time histories analysis were performed.

Structural Analysis

Four alternative methods were used to perform structural analysis of the structure (FEMA-350 2000). These were Linear Static, Linear Dynamic, Push Over and Nonlinear Dynamic Analysis. In a linear static analysis, an elastic material model of the concrete frame was created in Visual Analysis software. Furthermore, two set of loads were created for analysis. In first set of loads the maximum of all the force time histories were applied to the structure. While, in the second set the mean of all the force time histories is calculated and applied to structure.

Response to these load sets is measured in terms of drift at top corner (node 52). The results of the linear static analysis are to be used as a benchmark for response from dynamic analysis.

Pushover analysis or Nonlinear Static analysis is a procedure in which a monotonically increasing load is applied to structure until it fails. In this study, loads were applied at the nodes on one face of the structure and responses were measured. This pushover analysis was performed to obtain the load at which material will begin to yield.

As discussed earlier, all 322 load time histories combinations were applied to the model. Dynamic analysis was performed using the model created in OpenSEES. The elastic material model of concrete was used in Linear Dynamic analysis and nonlinear material model was used in nonlinear dynamic analysis. Force time histories were applied to respective nodes in the model. The responses to dynamic analysis are measured in terms of displacement at node 52. Results of the analysis are further discussed in result section.

Before proceeding to structural analysis results, it is should be noted that, this is a parametric study and thus certain parameters are assumed in the study. The wind loads were applied to structure at the sampling rate of 22 data per second. While the wave data was applied at the rate of one data per second. The wind forces calculated in the equation 1 was applied to the structure as calculated. According to Wu et al, (2006) after wave break at shore, the maximum setup wave that reaches inland structures is only 10-20%. Hence, it was assumed that only 20% of the wave force generated at the shore would reach the structure.

CHAPTER FOUR:

RESULTS

Probability Distribution Analysis

Probability distribution analysis was performed for all the hazards chosen for this study, namely Wind Speed, Surge Height, and Significant Wave Height. In this study, wind and wave height were treated as an independent event and surge height was dependent on V_t Batts 1000 year simulated maximum non-directional wind speed data was fitted with various distributions to estimate the most suitable distribution. For Miami-Dade, the location selected for this study, Rayleigh distribution best describes the distribution of data. The CDF of the data distribution is plotted below (Figure 16). The maximum wind speeds for 20 and 50-years return period were 99.4mph and 116mph respectively.

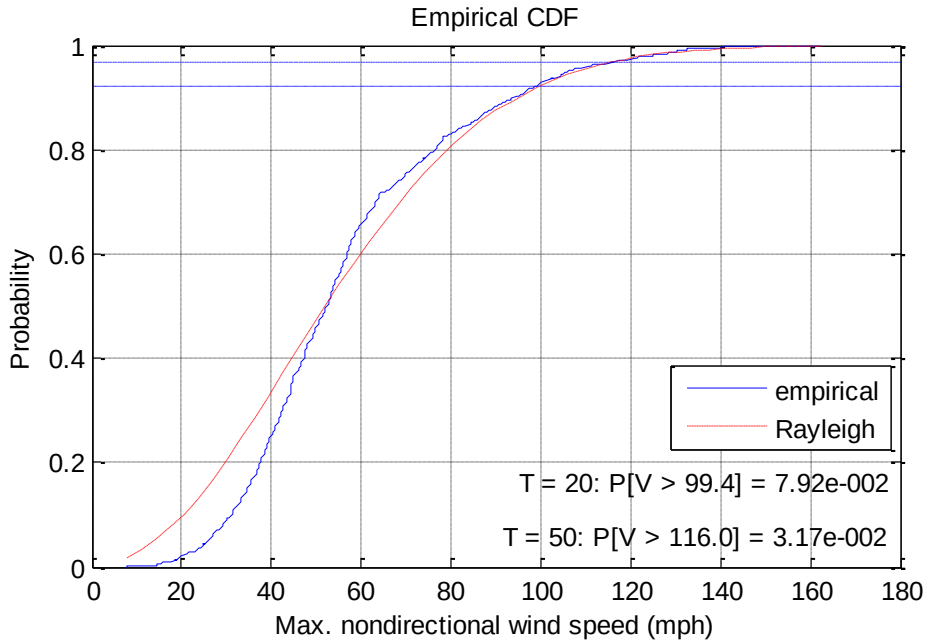

Figure 16 CDF of 1000 year simulated maximum non-directional wind speed data

Once aware of the mean wind speed distribution, the probability distribution of surge data was computed. In this study, surge data was generated using category of hurricane and translational wind speed using SLOSH. The surge values for each category of hurricane at Miami Dade were estimated. All these surge heights were then fitted with suitable distribution for each category. Gumbel distribution was discovered to be the most suitable for the probability distribution of surge height for all categories of responses for Miami Dade. The CDF of surge height for category 3 hurricane is plotted below (Figure 17).

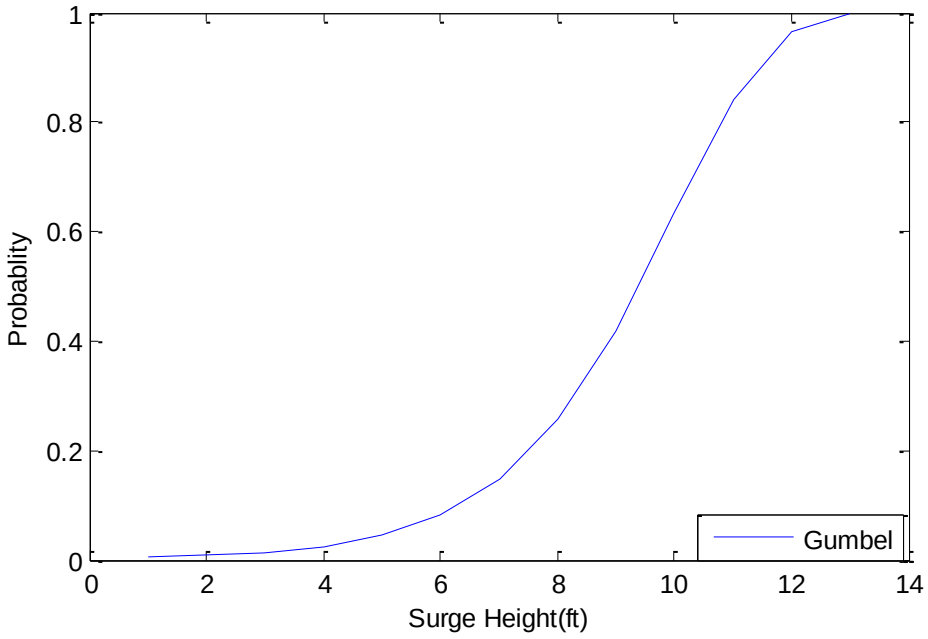

Figure 17 CDF of Cat-3 Storm Surge

In this study, surge heights are dependent on the mean wind speed category. The joint probability of the two distributions is plotted to find the mutual occurrence of two hazards.

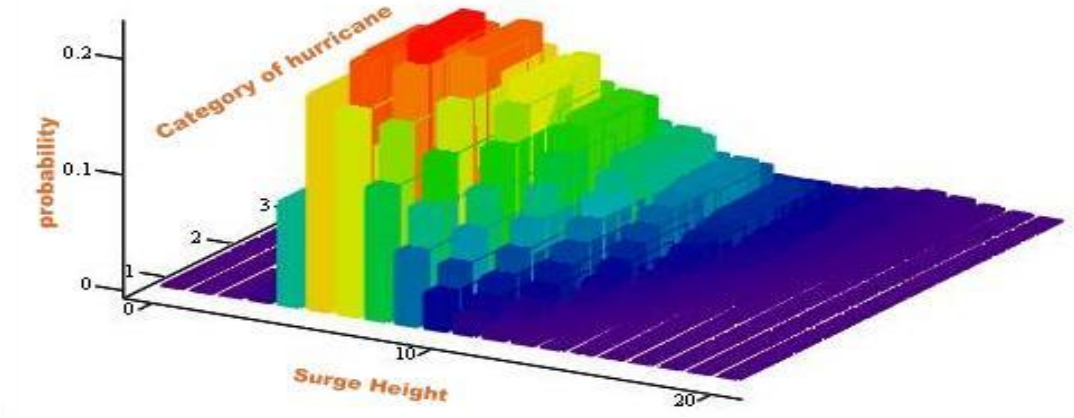

Figure 18 Joint probability plot for Mean wind speed and surge height

This joint probability plot (Figure 18) will be used to select the right combination of wind and surge loads for the structural analysis. For 50-year return period a maximum mean wind speed of 116 mph, a surge height of 8ft was found to have a maximum probability of 0.2. This combination of maximum wind and surge will be used in response probability analysis. Similar to surge height, probability analysis of wave height was performed. It was ascertained that the log normal distribution was the best fit for the significant wave height data. Joint probability distribution analysis was performed and result is presented below (Figure 19)

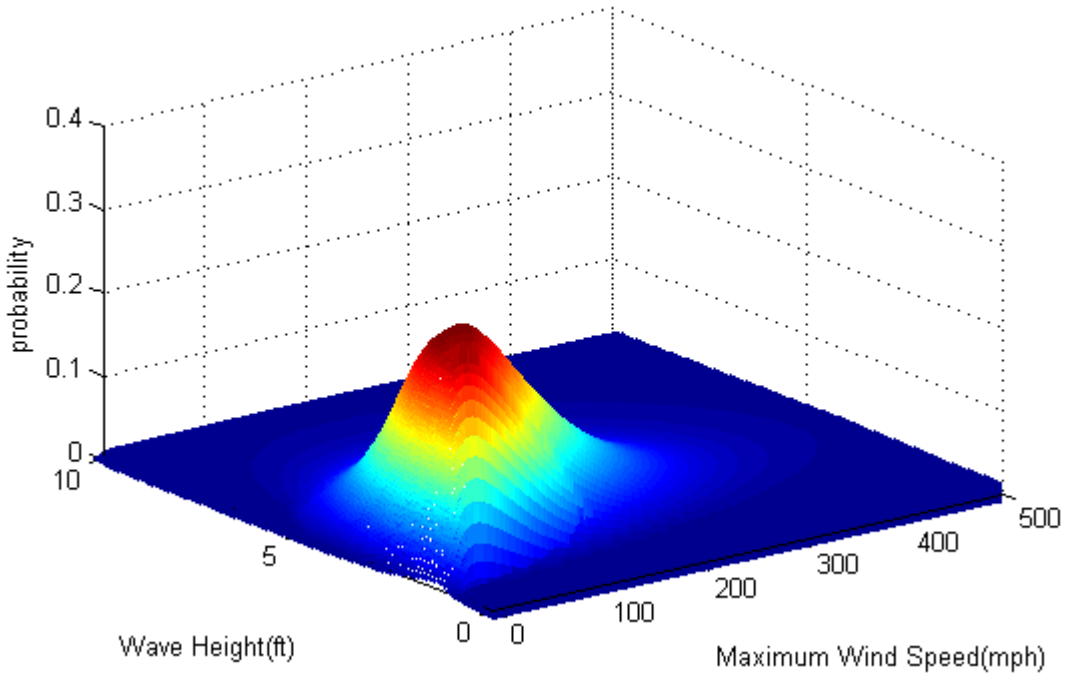

Figure 19. Joint probability plot for mean wind speed and wave height

Spectral Analysis

To create the frequency spectrum of the hurricane wind time histories, Welch method with hamming windows was employed. The spectrum response was compared with other researchers (Yu et al., 2008) and Schroeder et al., 2002) for correctness of the wind time histories data. The wind tunnel test had a sampling frequency of 500 samples per second, which was converted into equivalent full model sampling rate of 22 samples per second. The power axis of the spectrum was normalized by the frequency and variance of data. While, the frequency axis was normalized by the mean of data. The frequency spectrum is shown below in figure 20. It was observed that the dominant frequency were lower than that recorded during hurricane event (Yu et al., 2008)

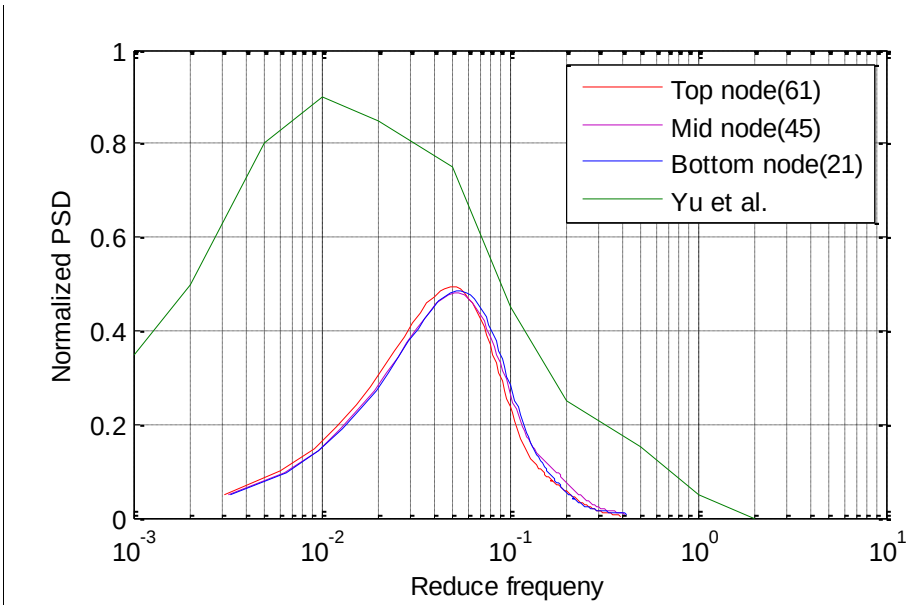

Figure 20 Power spectrum of recorded wind speed data at edge column

After comparing the spectral response to Yu et al (2008), it was established that the shape of normalized spectra of wind tunnel time histories was same as hurricane wind spectra. The dominant frequency of the wind tunnel spectra were slightly higher but less energy than that of hurricane wind spectra. The variation in spectral properties could be attributed to the difference in normalization factor used. These time histories were then used to perform structural analysis without any modification.

Auto and cross correlation of the time histories were analyzed to find spatial and temporal correlation of pressure time histories. It was observed that wind speeds were not periodic in nature (Figure 21) and there was only one dominant wind frequency.

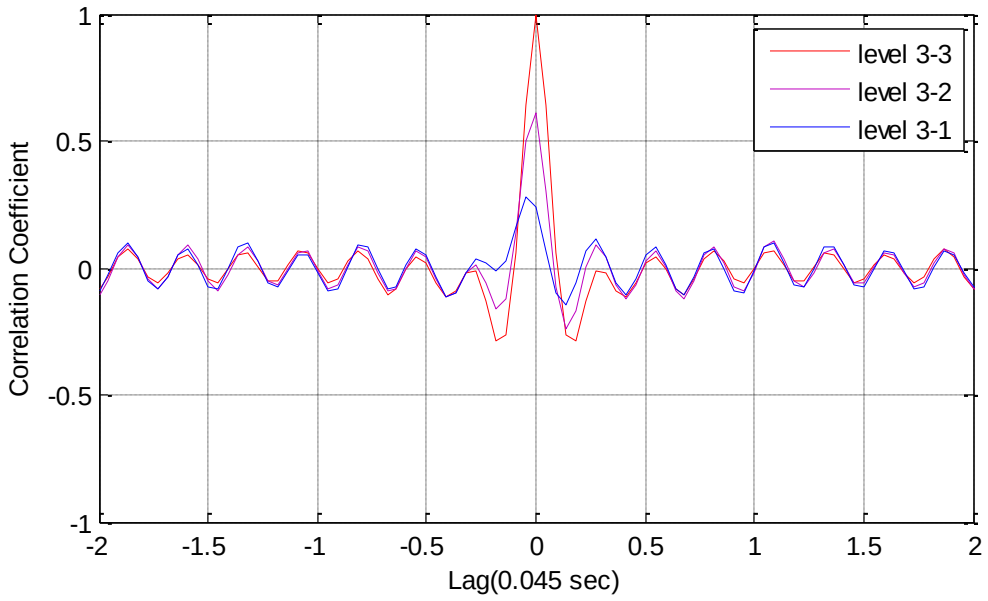

Figure 21 Variation of auto and cross correlation with time lag of 0.045sec on windward side

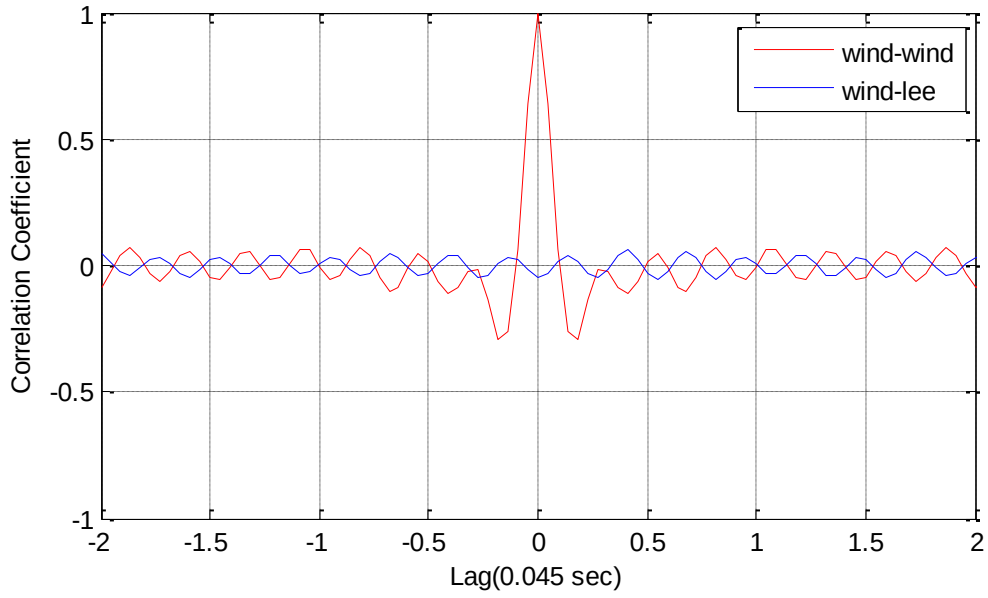

Figure 22 Variation of auto and cross correlation with time lag of 0.045sec on windward and leeward side

Furthermore, it was observed that time histories on windward and leeward sides of the structure were negatively correlated (Figure 22), whereas time histories of wind on windward side were positively correlated. The magnitude of cross correlation was same in both cases.

There were four wave time histories (A, B, C and D) available for spectral analysis. Wave time histories A and B were generated by simulation and C and D were generated in the Lab basin test. The key parameters of the seed wave were same for both simulation and basin test. The input to the seed wave of simulation consisted of JONSWAP spectrum with a wave height of .12m and period of 1.8 sec. Before using these time histories for structural analysis, spectral analysis of wave time history was carried out. The dominant frequencies and their energy were compared with the sea wave spectrum for worse sea scenario (Fernandes et al, 2008). It was determined that the frequency (Figure 23 and Figure 24) and power of the spectrum were same as worse case scenario of sea wave.

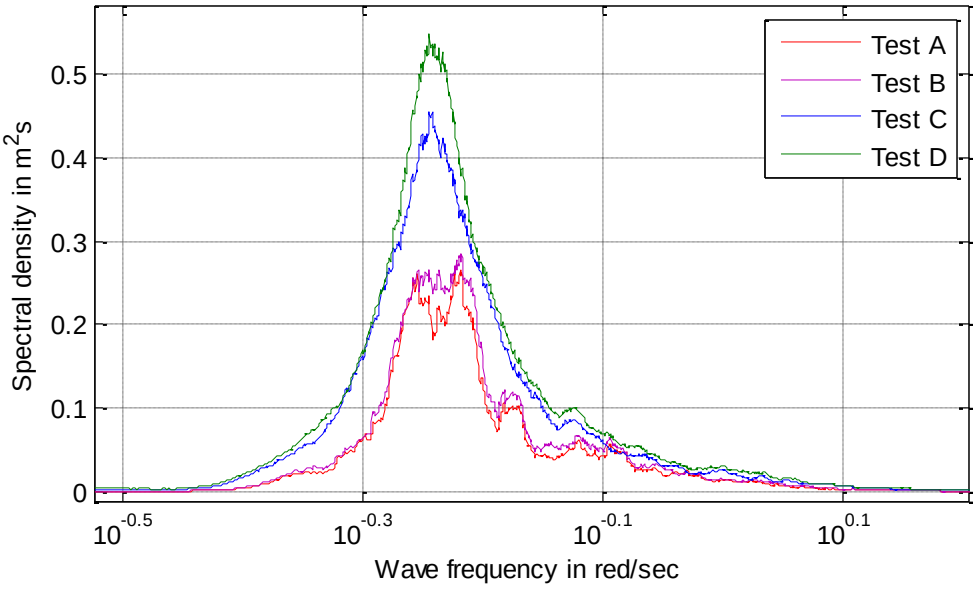

Figure 23 Wave spectra for wave generated from simulation and laboratory test using input wave height 0.12m and peak period 1.8 seconds

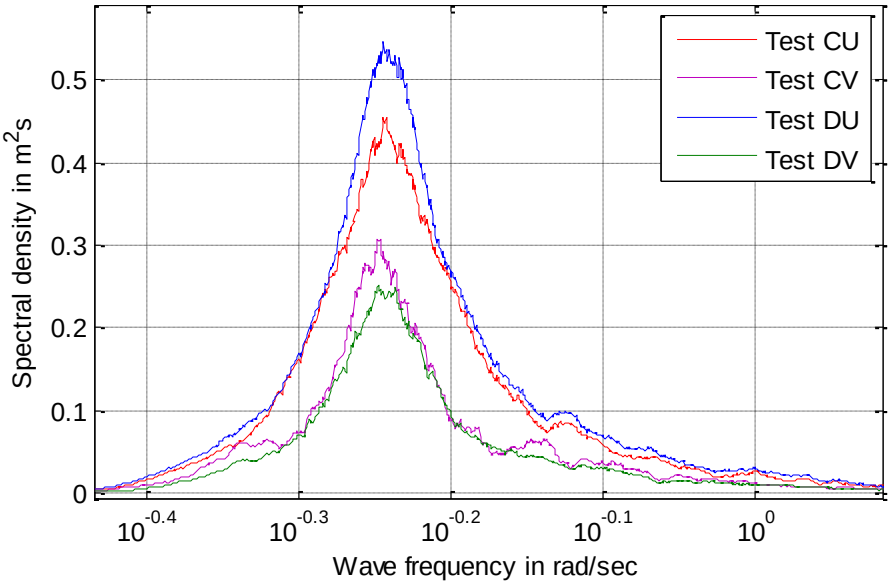

Figure 24 Wave spectra for wave generated laboratory test at CHL using input wave height 0.12m and peak period 1.8 seconds

Auto and cross correlation analysis results of the wave time histories were significantly different from that of the wind. The wave data was highly correlated in the time domain as expected. The correlation coefficient between the two different wave time histories (C& D) were positive in time domain (Figure 25), but was very low compared to the auto correlation coefficient

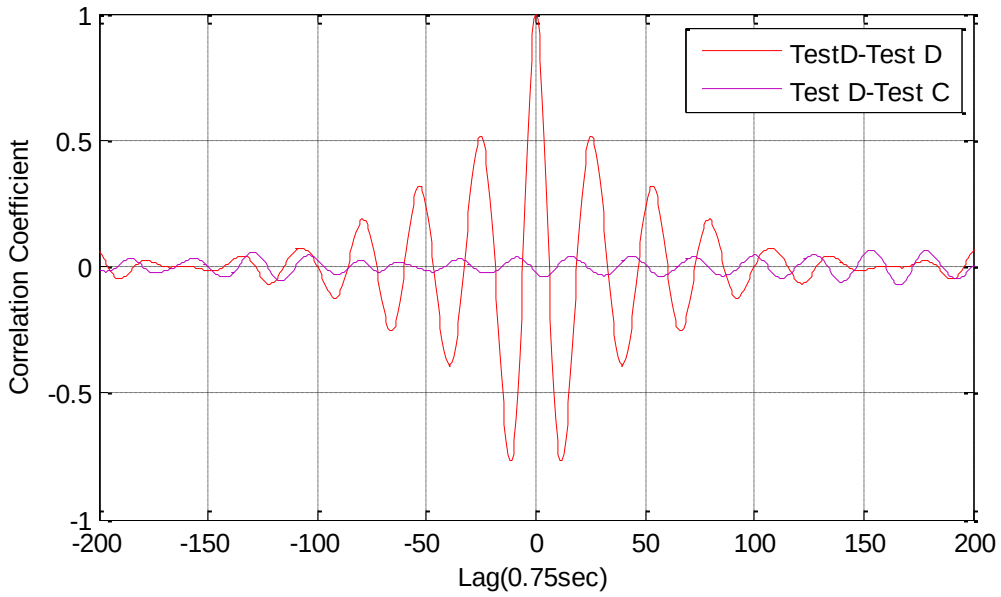

Figure 25 Variation of auto and cross correlation of wave data with time lag of 0.75sec for lab test C and D

Structural Analysis

The results of linear static analysis were used as an estimate for the response of the time history analysis. These results were then compared with the linear and nonlinear dynamic responses to find amplification and de-amplification appearing in the time histories analysis. It was observed that in all the cases of static and dynamic analysis, the responses from dynamic analysis were greater than static analysis cases.

In the push over analysis, the structure was pushed laterally up to 10% of drift and response was measured. The moment curvature plot of response for three levels of floor columns is shown below. Push over analysis showed that the bottom column begins to yield first as expected. No yielding happened at the second and third floor for 10% drift. This plot was used in the nonlinear dynamic analysis for determining the yielding point.

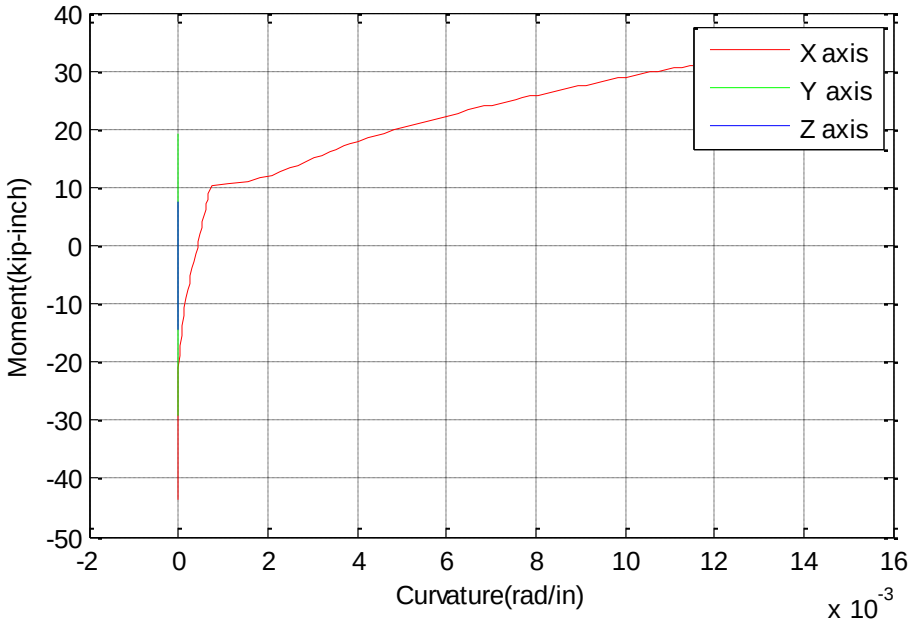

Figure 26 Moment Curvature at the bottom of column for three directional coordinates of building on windward side

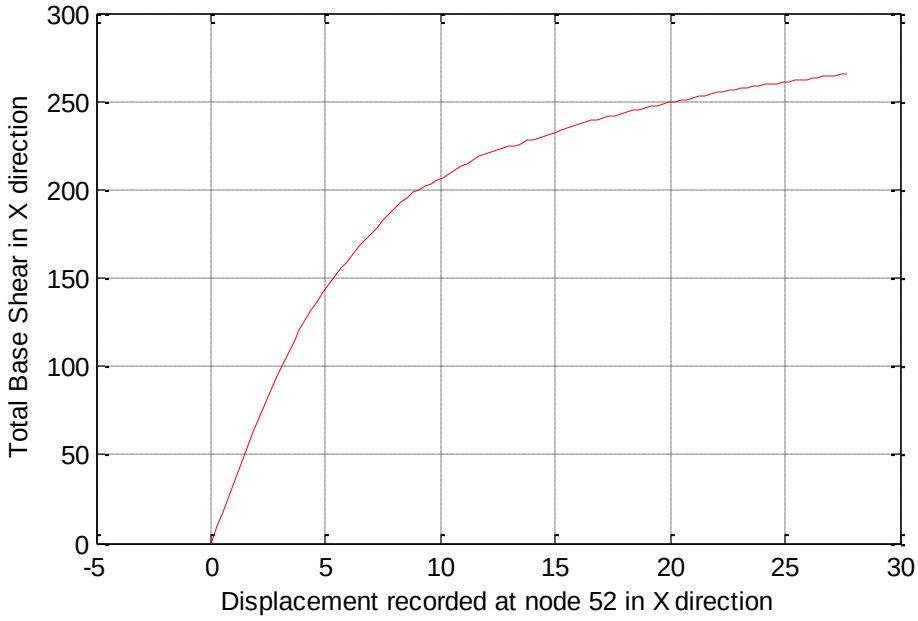

Figure 27 Total base Shear Vs Displacement at node 52 in X direction

Not all 322 cases of dynamic analysis are listed in the result section, but the trends in responses are presented in detail. Results of parametric study are discussed in three subsets. In the first subset, the variable parameter was mean wind speed and preset parameters were surge and wave heights. The general trend of displacement responses are presented followed by the plot of base shear vs. displacement. The responses were further analyzed by power spectrum of the response time histories. In all the cases, the comparison between linear and nonlinear material model is made. In next sub set, the surge height varies while mean wind speed and wave height remain constant. Results are presented in same order as that of the first subset. In the third and last sub set, both the mean wind speed and surge height are constant and the wave height is a variable parameter.

The entire dynamic analysis results are identified by a case numbers. Each case number has seven digits preceded by the material model label LN or NL, which stands for linear and nonlinear model respectively. The first three digits of case number indicate the mean wind speed. The following two digits specify surge height and the last two digits denote wave height. For example, LN1000805 means linear model with mean wind speed of 100 mph, surge height of 8 ft and wave height of 0.5 ft. Due to the presence of steel reinforcement the nonlinear model is slightly stiffer then linear model. Hence, as long as nonlinear model section is not yielding, the response from it will be less than linear model. All the results presented have their nonlinear material model yielded.

Table 7 Load case used in the analysis

Case Number	Legend	Explanation
NL1000805	LN(linear dynamic), NL(nonlinear dynamic), LS(linear static),NS(nonlinear static)	Material model
NL**100**0805	080, 100, 120, 140, and 160 mph	Wind speed
NL100**08**05	02, 04, 06, 08, and 10(ft)	Surge height
NL10008**05**	05, 10, 15, 20, and 25 (ft/10)	Wave height

Before investigating the responses, comparison of linear vs. static was done to see evidence of amplification in dynamic analysis. Two cases NL0800805 and NL1600805 are presented as Figure 28 Nonlinear Dynamic response Vs linear static response case NL0800805and Figure 29. It appears the there is no major dynamic amplification measured due to increasing the magnitude of force time history. The average dynamic difference factor of approximately 0.3-1.4 was observed in all the cases of linear and nonlinear dynamic analysis

(Figure 30 and Figure 31). The increase in the displacement response value was attributed to the yielding of structure and not because of dynamic amplification. Comparison between linear static and nonlinear dynamic was done to see the change in response due to the material model. It was observed that most of increase in response was due to material model yielding (figure 28 and Figure 29). Cases were the material model did not yielded the static responses was grater then dynamic response and vice versa.

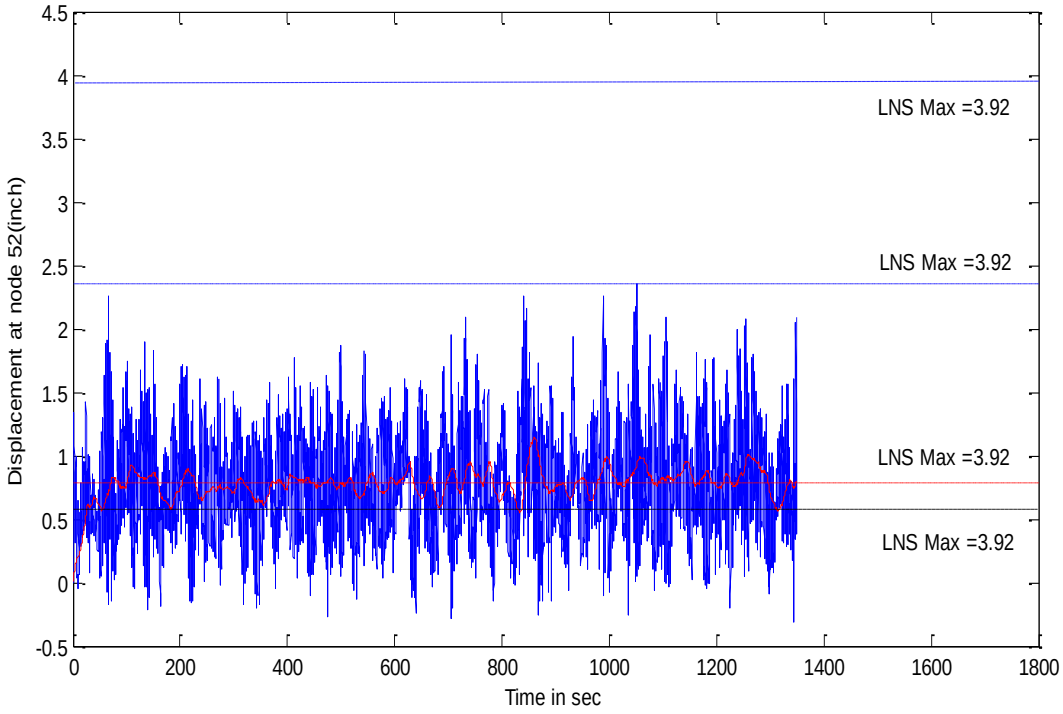

Figure 28 Nonlinear Dynamic response Vs linear static response case NL0800805

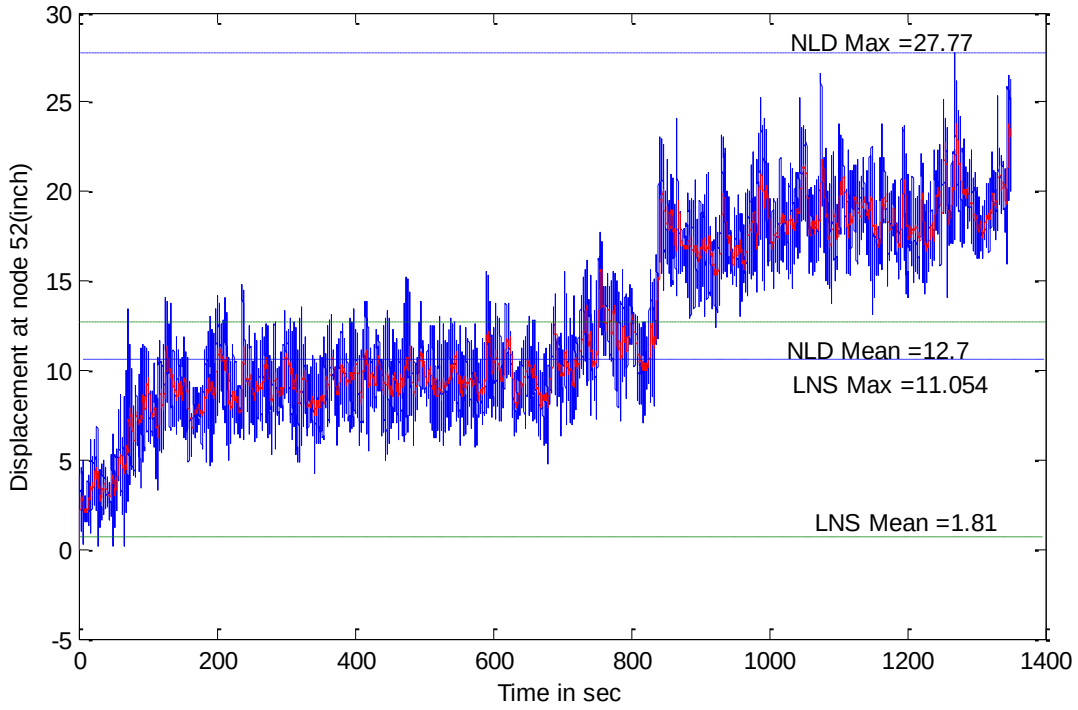

Figure 29 Nonlinear Dynamic response Vs linear static response case NL16000805

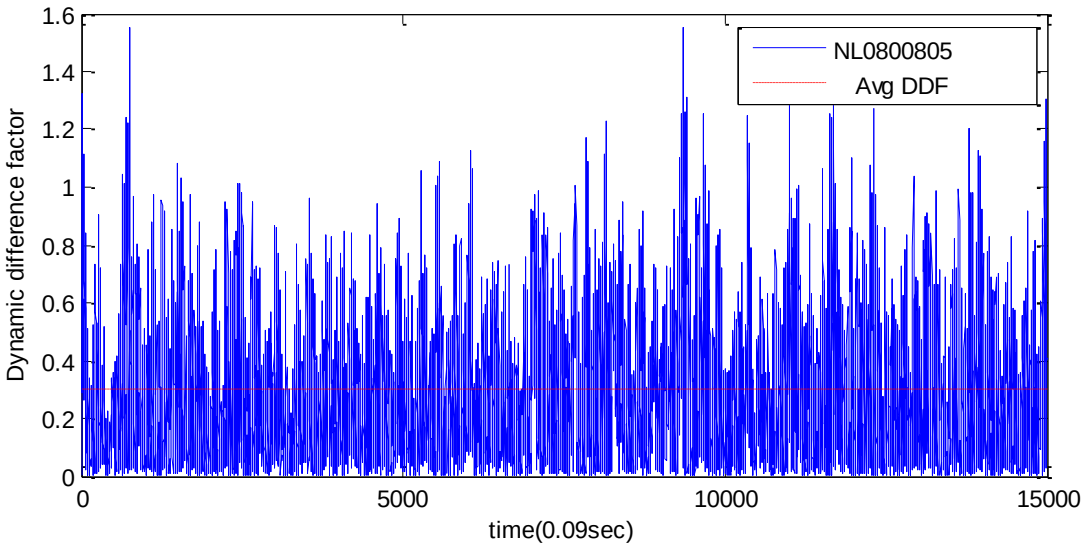

Figure 30 Dynamic amplification factor for load case NL0800805

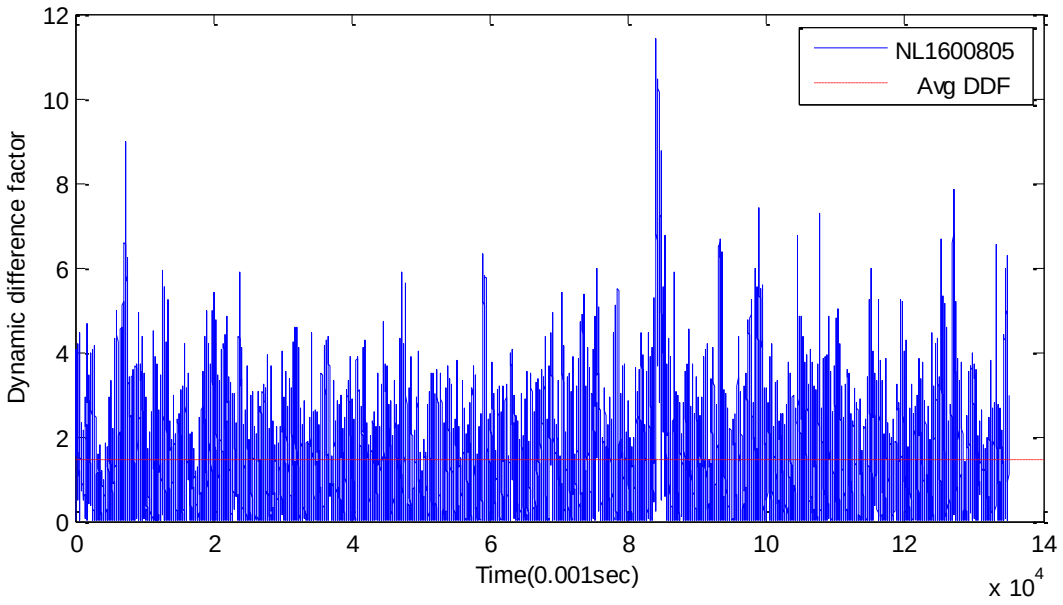

Figure 31 Dynamic amplification factor for load case NL1600805

For first subset, mean wind speeds of 80, 100, 120, 140, and 160 (mph) are applied to the model with a constant surge/wave of 8.5 ft in all the cases. As seen in Figure 32 Displacement trend for variable mean wind speeds and constant surge and wave height.the mean and maximum displacement of nonlinear dynamic analysis are always higher than that of linear dynamic response. As seen from the trend the maximum responses are varying almost exponentially with increase of mean wind speed. In comparison to the mean displacement response are varying linearly with increase of mean wind speed.

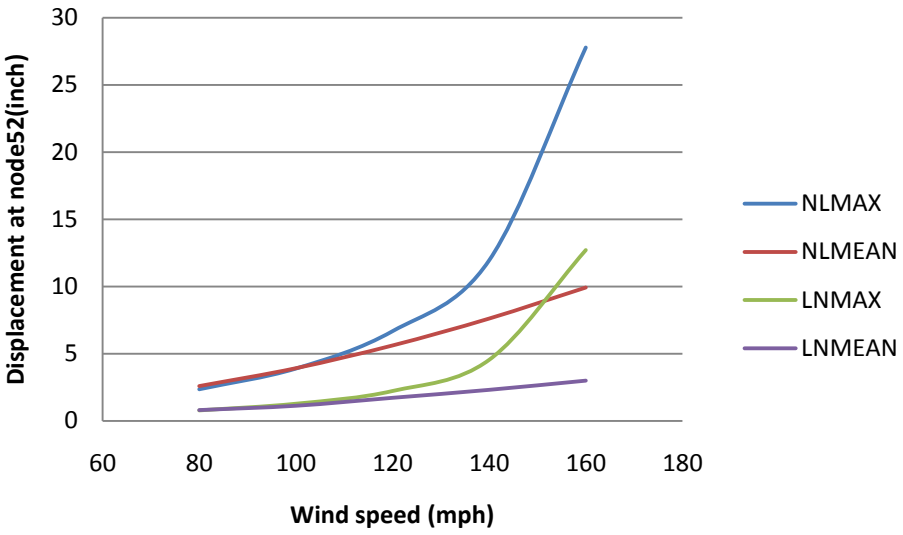

Figure 32 Displacement trend for variable mean wind speeds and constant surge and wave height

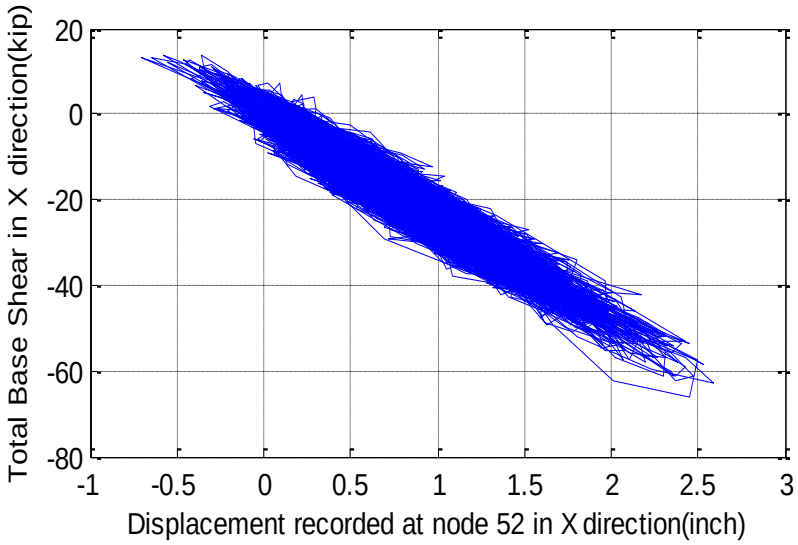

Figure 33 Base shear Vs Displacement for load case LN0800805

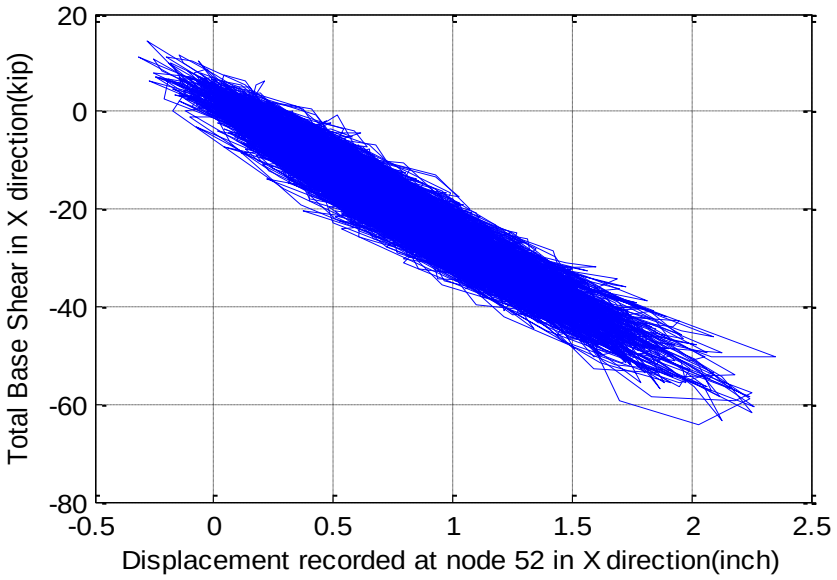

Figure 34 Base shear Vs Displacement for load case NL0800805

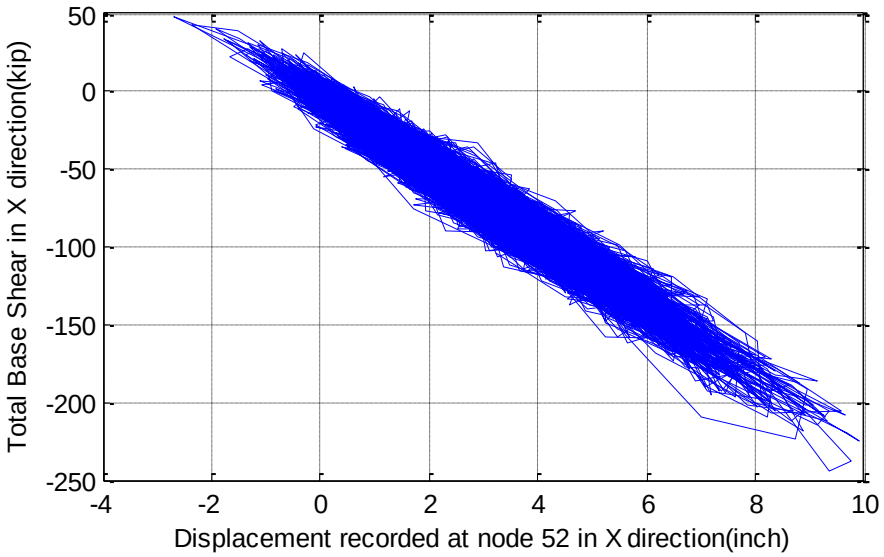

Figure 35 Base shear Vs Displacement for load case LN1600805

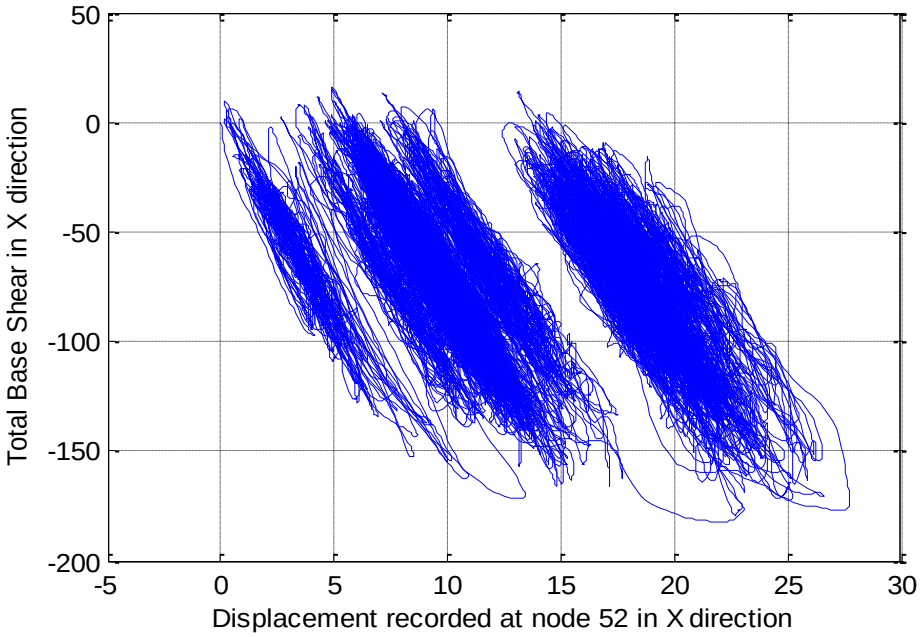

Figure 36 Base shear Vs Displacement for load case NL1600805

Base shear vs. displacement shows the occurrence of yielding in the model. In the event whereby yielding does not occur the base shear plot is same for linear as well as nonlinear material as observed in figure 33-36 for analysis case NL0800805. Ideally, the base shear vs. displacement for linear material should be a straight line, but the inertia of a structure introduces noise in the response plot. For the case NL1600805, there are three clear loops showing that the material has yielded at least twice.

Dynamic response spectrum of a structure consists of two components, background response and resonance response. Background responses are lower frequency content of power spectrum compared to natural frequency system. They have been disregarded in this discussion. Normally, dynamic resonance response of low-rise structure is insignificant, but for this study, it was significantly high. This could be attributed to the fact that the natural frequency of the

structure is close to 1 Hz, hence it is behaving like a flexible building. Usually the dominant frequency of wind is less than the lowest natural frequency of structure. However, in this study the dominant frequency of wind and natural frequency of structure are very close. In the response spectrum (Figure 37, Figure 38 and Figure 39), it was observed that structure is responding only at its first natural frequency

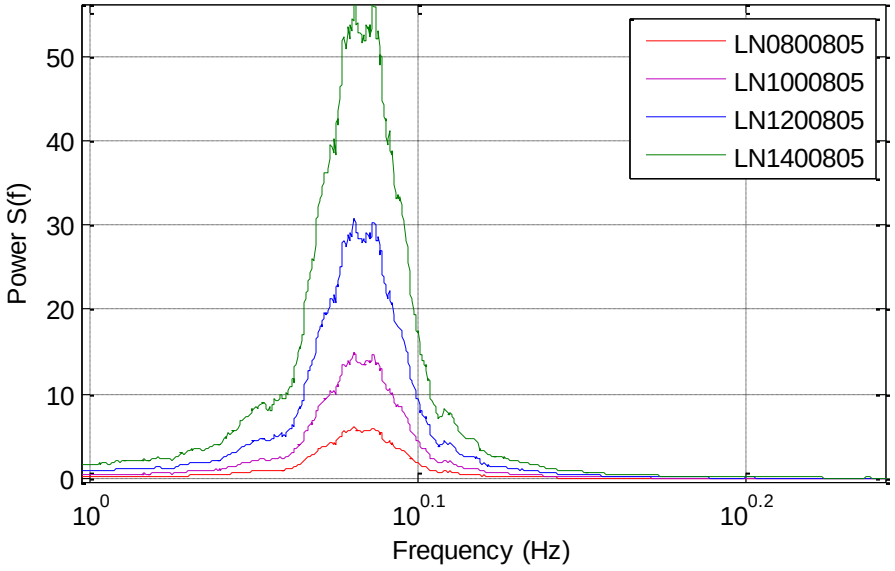

Figure 37 Power spectrum of linear material model response for variable wind speed and constant surge and wave height

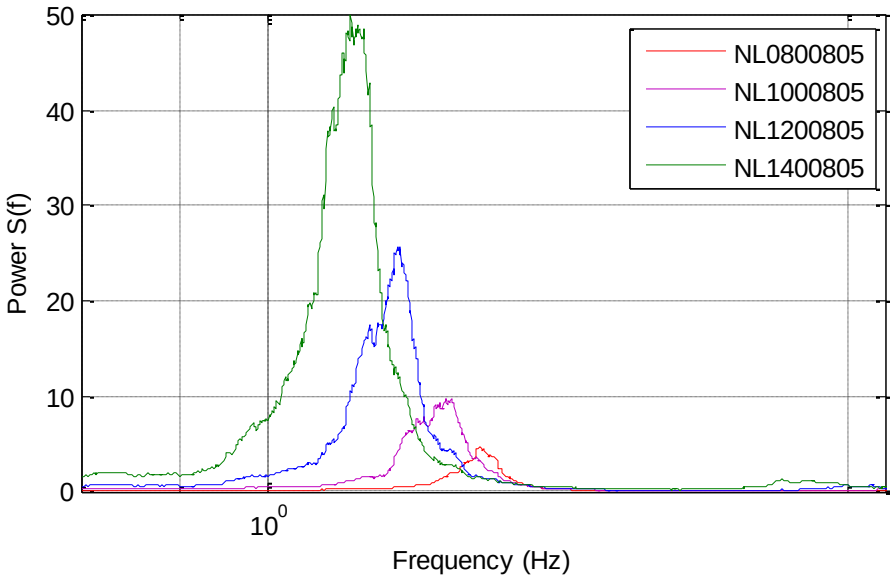

Figure 38 Power spectrum of nonlinear material model response for variable wind speed and constant surge and wave height

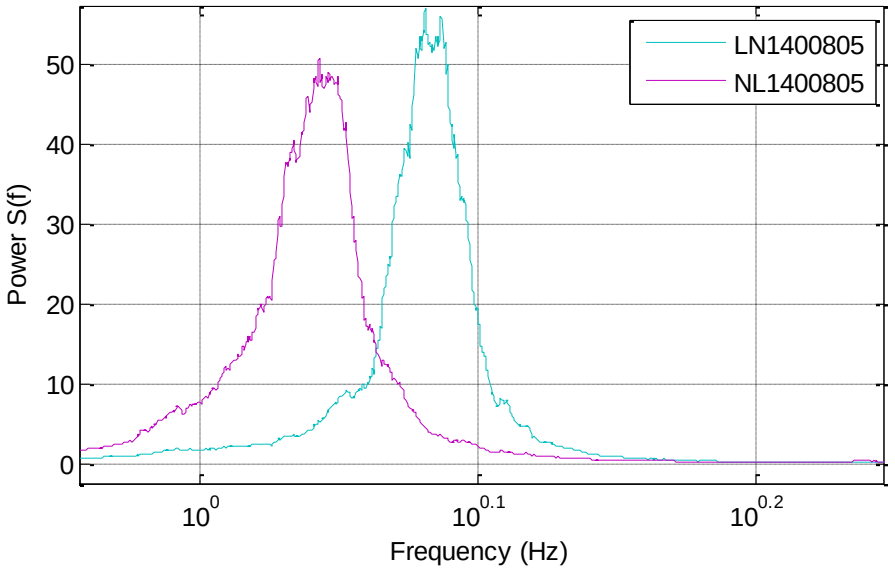

Figure 39 Power spectrum of linear and nonlinear material model response for constant wind speed and surge and wave height

As can be noted in Figure 37, the there is a direct relationship between wind speed and frequency response. Hence, increase in one leads to other. For the two different material models, it is observed that the frequency response of linear model is higher than nonlinear model response. This could be explained by change in the stiffness of structure, which furthers leads to a change in the natural frequency of the model. The peak response frequency of nonlinear spectrum appears to occur slightly lower than the natural frequency of structure. This could be attributed to a decrease in stiffness of structure, resulting into lowering of natural frequency of structure.

In the second subset the wind speed of 120mph, wave height of 1.5ft and surge height of 2, 4, 6, 8 and 10 ft are applied. The displacement responses from the nonlinear model are relatively higher than that of linear model (Figure 40). In this subset, it is observed that the mean of nonlinear model response is not varying linearly as in first subset. No change was observed in the spectrum of linear analysis compared to the first subset (Figure 41). The dominant frequency in the spectrum was reducing with increase surge height (Figure 42). This could be attributed to the fact that the structure is yielding that leads to change in natural frequency of structural system.

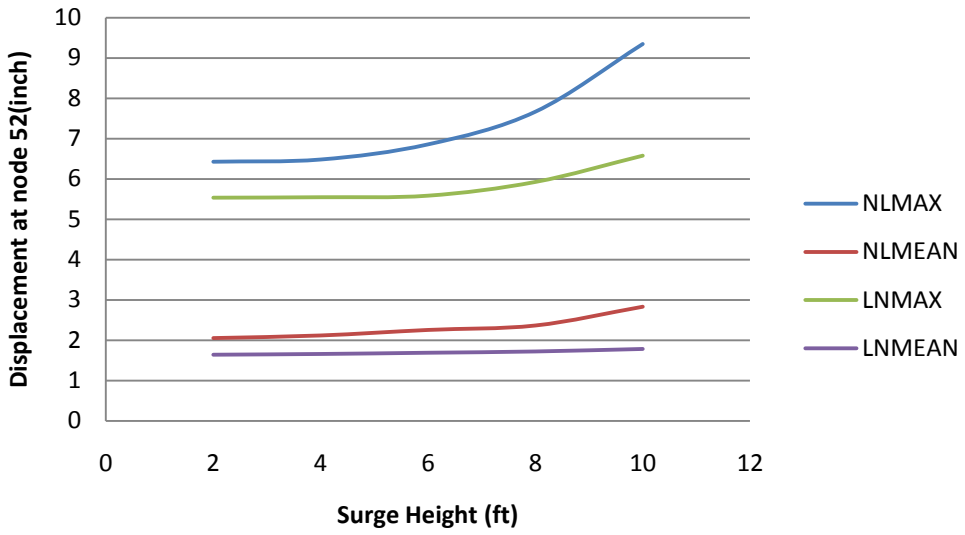

Figure 40 Displacement trend for variable mean surge height and constant wind speed and wave height

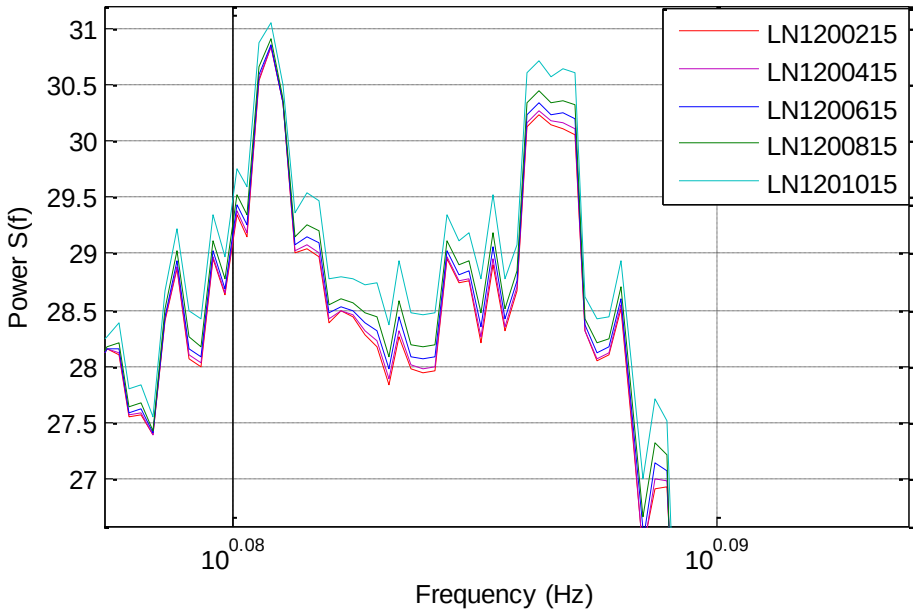

Figure 41 Power spectrum of linear material model response for variable mean surge height and constant mean wins speed and wave height

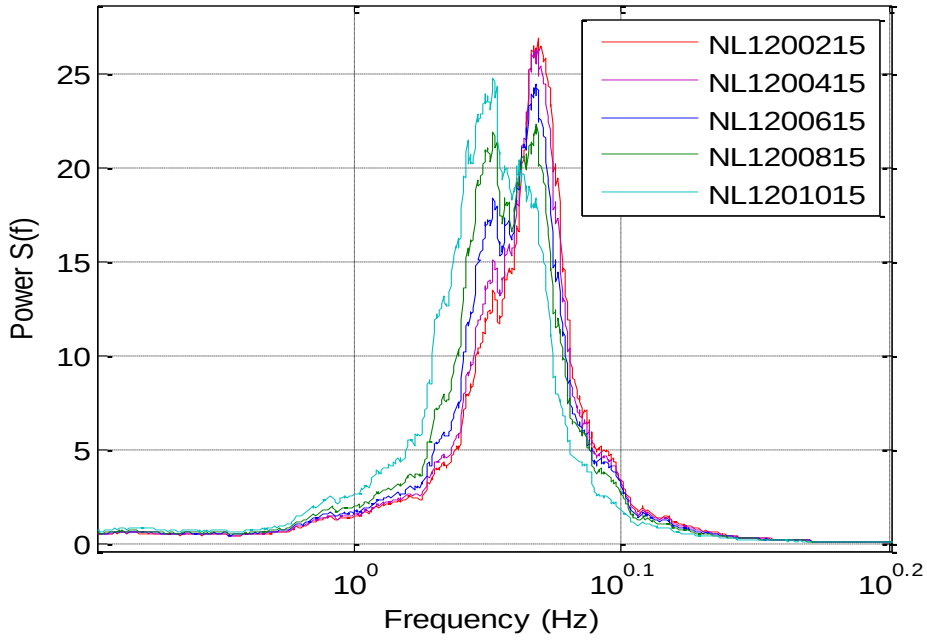

Figure 42 Power spectrum of nonlinear material model response for variable surge height and constant mean wind and wave height

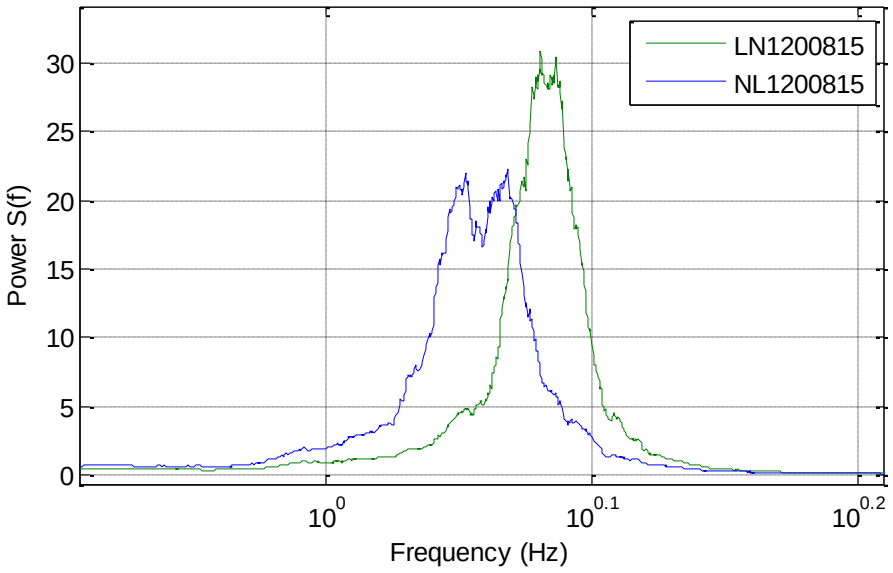

Figure 43 Power spectrum of linear and nonlinear material model for constant mean wind speed, surge height, and wave height

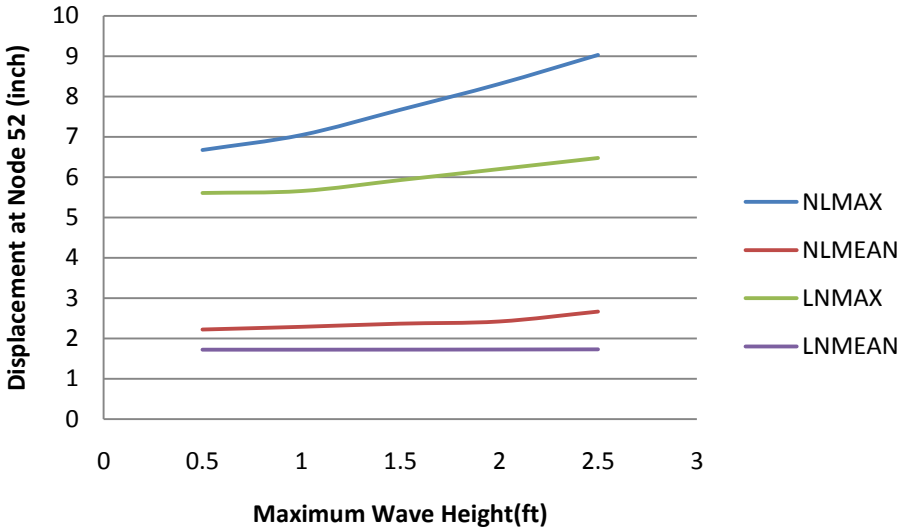

Figure 44 Displacement trend for variable wave height and constant wind speed and surge height

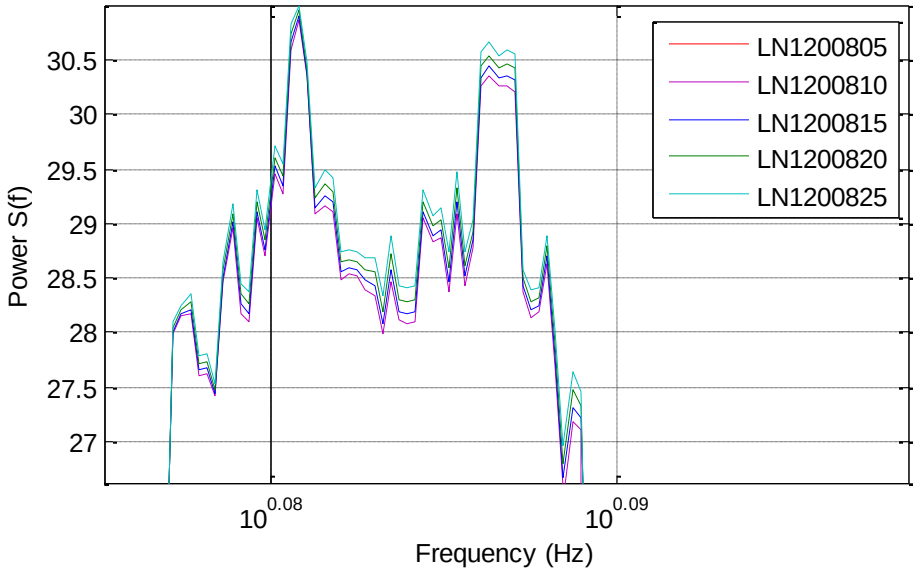

Figure 45 Power spectrum of linear material model response for variable wave height and constant mean wind speed and surge height

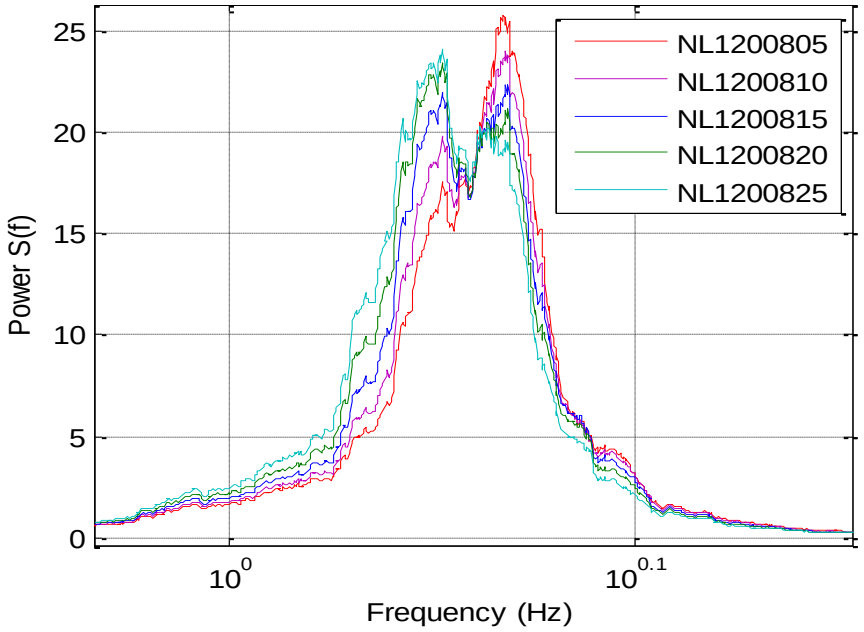

Figure 46 Power spectrum of nonlinear material model response for variable wave height and constant mean wind speed and surge height

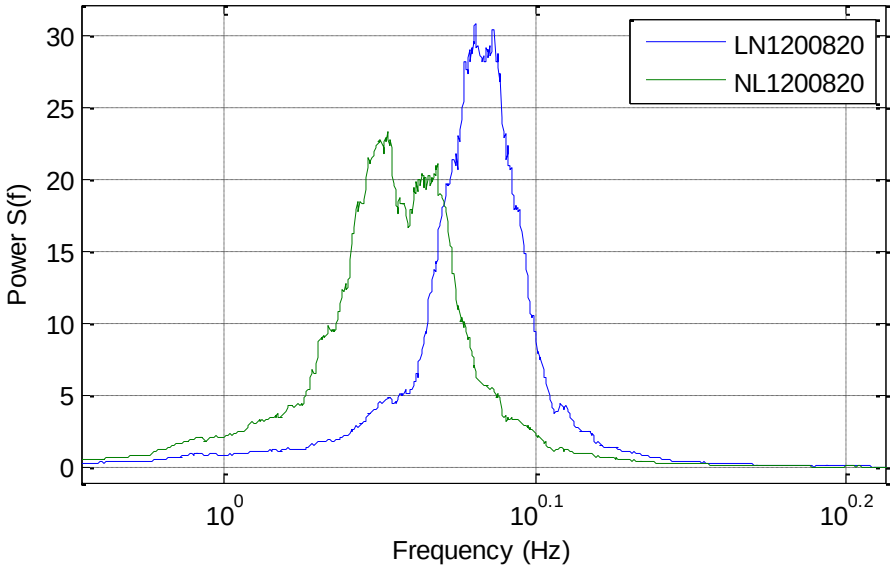

Figure 47 Power spectrum of linear material model response for constant wave height, mean wind speed and surge height

In the last subset the wind speed of 120mph, surge height of 8 ft and wave height of 0.5, 1.0, 1.5 2.0, and 2.5ft and are applied. The displacement responses from the nonlinear model are relatively higher than that of linear model (Figure 44). In this subset, it is observed that the mean of nonlinear model response was varying linearly. No major change was observed in the spectrum of linear analysis. Change in the dominant was observed with the increase in the wave height

Response Probability Analysis

The above-mentioned three subsets illustrate the variation in the trend of structural response conditioned on various hazard parameters. All three scenarios have just two realizations for any given load combination. However, those are insufficient to predict the uncertainty in response. Therefore, to generate more realizations for a given mean wind speed and surge/wave height, it is essential to create several time histories and consequently, these will produce different responses to same load scenario. Also, as mentioned in the Methodology section, 72 load cases with wind speed of 100mph, surge height of 4ft, and maximum wave height of 1.5 ft were applied and responses was recorded.

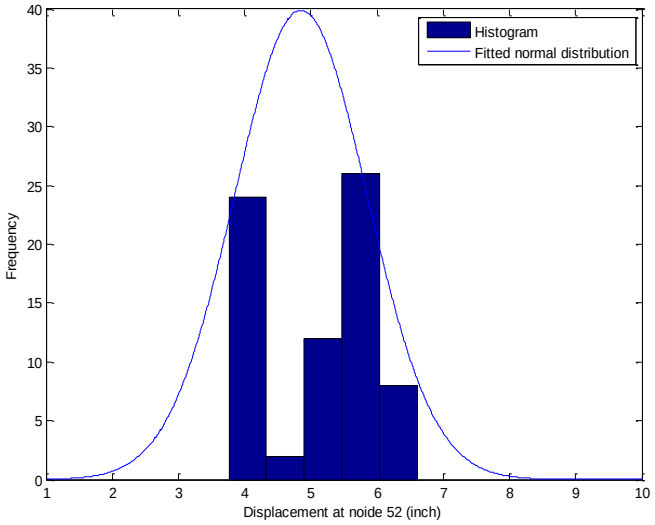

Figure 48 Histogram of response probability analysis for additional 72 load cases.

Due to the lack of sufficient time histories, there were not enough data points in the histogram to fit any distribution to it as seen in Figure 48. Owing to the inconsistencies in histogram data, it was assumed that the response was following a normal distribution with a mean of 4.85 ft and standard deviation of 1ft. from this probability plot. It is important to reiterate here that the response PDF plotted above was generated for one load combination, out of 125-load combination discussed above. If this process was done for all 125, cases there would have be 125 responses PDF's. Hence each load case would have it own set of responses and each response will have certain probability. This knowledge of responses and there probability of occurrence can then be mapped to damage and subsequently to losses. This awareness of hazards, responses, damage and losses will empower the owner and designer to make discussion regarding the structure in a most efficient way

CHAPTER FIVE

CONCLUSION

This focus of the study was to quantify the uncertain response of structures to the predominant hazards associated with hurricanes using a performance-based engineering methodology. Various hazards associated with hurricanes were identified. The three most critical hazards, namely wind speed, wave, and surge height were selected for study. The most challenging part of this study was generating hurricane hazard data and finding a correlation between them. Two sets of data namely annual (extreme value) data and time history data were required for the analysis. Annual hazard data of wind speed, surge height, and wave height were generated using NIST, SLOSH, and NOAA data sources respectively. These hazards were quantified in a probabilistic manner. The Rayleigh distribution best described 1000 year simulated data of wind speed, whereas the Gumbel distribution and lognormal distribution were an appropriate fit for all surge responses for each category of hurricane and wave height data respectively. After probability distribution analysis, the joint probability of hurricane hazards was plotted to find the joint probability of occurrence of various hazards. It was established from the joint probability plot that for the fifty-year return period, wind speed of 116 mph, the surge height of 8 ft and wave height of 1.5 ft had maximum probability. This information could be used in the design of structures in the coastal region. It is important to reiterate that the above information is based on available resources and only valid for a specific location. This method of hazard probability analysis could be implemented for any other locations, given availability of marginal distribution of hazards for that location.

Generating wind and wave time histories was a difficult task as there were no recorded time histories of hurricane winds and waves available in the public domain. Therefore, wind

tunnel time histories were used for hurricane time histories of wind load, while laboratory basin wave time histories were used as hurricane wave time histories. There is a distinct difference between the dominant frequencies of time histories, turbulence characteristics, and physical structure of wind generated during real hurricane events and wind generated during wind tunnel tests. Additionally the dominant frequencies in wind generated from real hurricane events were lower than that of wind generated from wind tunnel tests.

No records of the time histories of hurricane waves could be found during the research. Hence, laboratory basin time histories were used without any modification. Prior to applying these wave height time histories for structural analysis, auto and cross correlation analysis were carried out to see how these time histories are correlated in space and time. The wave time histories have a very high auto correlation compared to the auto correlation in wind time histories. The cross correlation in wind time histories was also small compared to that of waves. As there was no significant correlation in wind time histories, hence real time histories from wind tunnel test were used for each node in finite element model. Since wave had a high correlation then same wave time history was used for all the nodes where wave was acting.

The structure used for this study was a common three-story concrete frame building. The first natural frequency of the structure was low (near 1.4 Hz) as no floor was modeled and frame sections were small. This resulted into a flexible building instead of a stiff low-rise building typical of masonry or concrete construction. Wind, wave, and surge loads in this analysis were applied both as static and dynamic forces to investigate the necessity of performing dynamic time history analysis. From the results it was concluded that the response from dynamic analysis vary from static response for mean wind speeds higher than 120 mph. Hence, dynamic analysis for wind loads is necessary where dynamic analysis results are not significantly affected by wave

loads as the tributary area is smaller compared to that of wind forces. Wind forces being closer to the natural frequency of the structure were able to generate dynamic response from the structural model as expected. If the natural frequency of the system would have been increased, less response will be measured but higher dynamic amplification will occur.

Time history analysis of the three-story concrete frame structure was performed using two different material models, namely elastic concrete material model and nonlinear concrete material model. Both, linear and nonlinear analysis of the structure was conducted to compare results and determine if it is useful to perform a nonlinear analysis for a given amplitude of loading or not. After performing the structural analysis, it was observed that the nonlinear analysis total responses were higher in comparison to the ones from the linear model for given hurricane hazard loads. This confirms that both linear and nonlinear analyses are essential for hurricane analysis. The responses in the structural analysis were mostly depending upon the material and section properties. The increase in the magnitude of wind load time histories did not caused any significant increase dynamic amplification of response. Thus, it could be concluded for hurricane hazards loads nonlinear dynamic analysis can get us best estimate of response.

This study was not a complete application of performance-based engineering but an attempt to create a methodology to answer the complex problem of multiple hazards from a hurricane perspective. It was learned from the study that no hurricane loads could be quantified in a prescriptive way as it depends on many factors. It was proved from a sample response probability analysis that for a given mean wind speed of 100 mph, surge height of 4 ft and wave height of 1.5 ft the response can vary from 1.5 to 8 inches. Each mean force could have multiple realizations of response time history. This makes it imperative to analyze hurricanes from a

performance-based perspective to answer the complex problem of multi hazards in field of hurricanes engineering.

CHAPTER SIX

FUTURE STUDIES AND RECOMMENDATIONS

This being an exploratory study, basic meteorological model such as Batts wind field model and mathematical SLOSH program were used. Throughout the course of this research, various advanced models of wind surge and wave were studied but due to lack of availability in public domain, they were not used. In future studies it is recommended to use the below mentioned advanced models. Vickery wind field model, ADCIRC and SWAN models are recommended for wind speed, surge height and wave height for inland location respectively. For the dynamic analysis, wind tunnel time histories with identical wind speed spectrum were used in this study. In future studies, it is suggested to use real time histories of hurricane wind. For generation of wave time histories it is suggested to do more laboratory basin tests with wide range of wave heights and periods. As explained previously in this study that the data used for structural analysis were not real hurricane recorded data but data generated from different sources. It is not necessary using a real hurricane data will change the results but it will definitely enhance the quality of results.

In this study, only three hazards associated with the hurricane are discussed. Other hazards like scour, wind/water debris, and flooding may also directly affect the response measured. It is expected that wind/water debris will affect the structure by damaging the building envelope that will create an internal pressure, which may affect the response of structure. Flooding will exaggerate the hydrostatic load on structure that in turn will increase the total global response of structure.

APPENDIX

ADDITIONAL RESULTS AND PLOTS

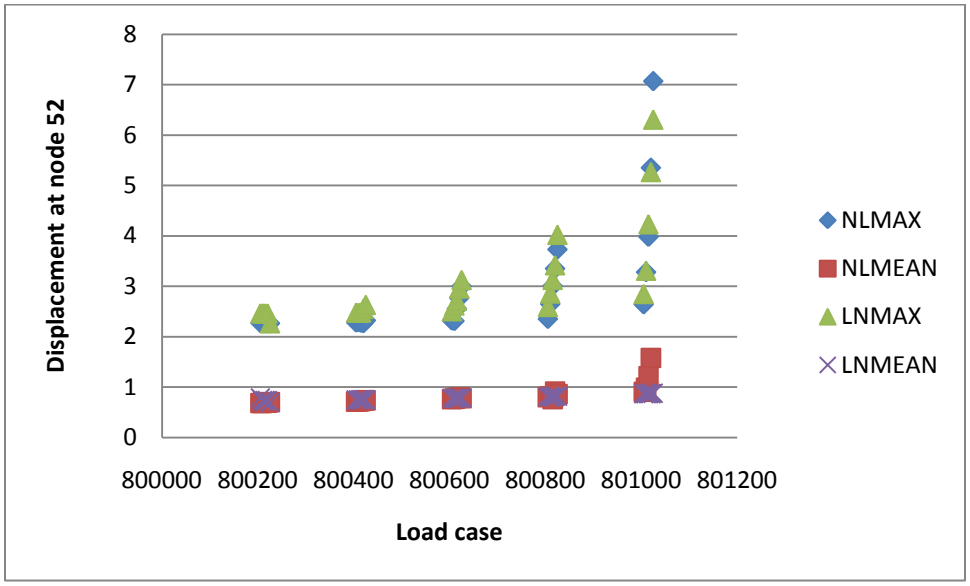

Figure 49 Trends of maximum and mean response of linear and nonlinear model for Mean wind speed of 80 mph

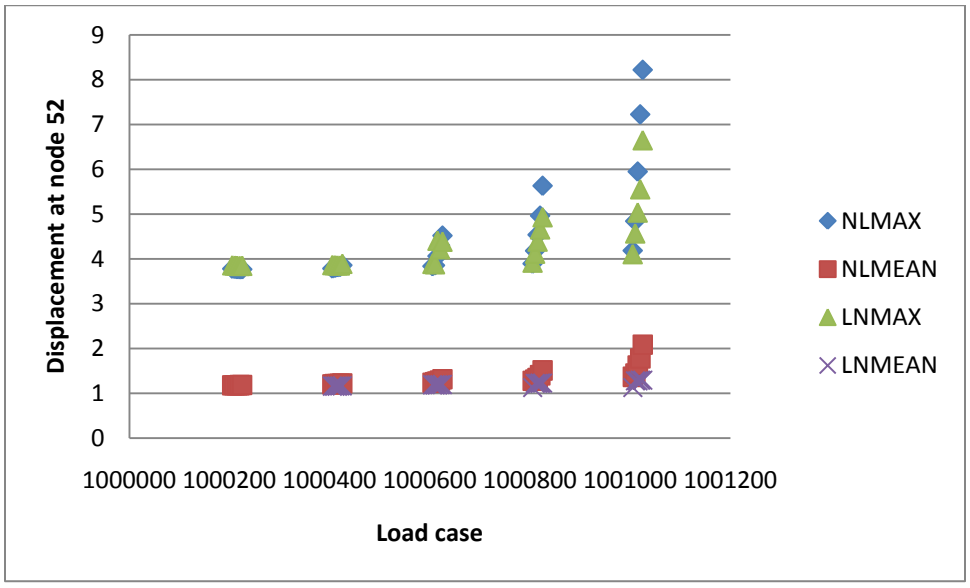

Figure 50 Trends of maximum and mean response of linear and nonlinear model for Mean wind speed of 100 mph

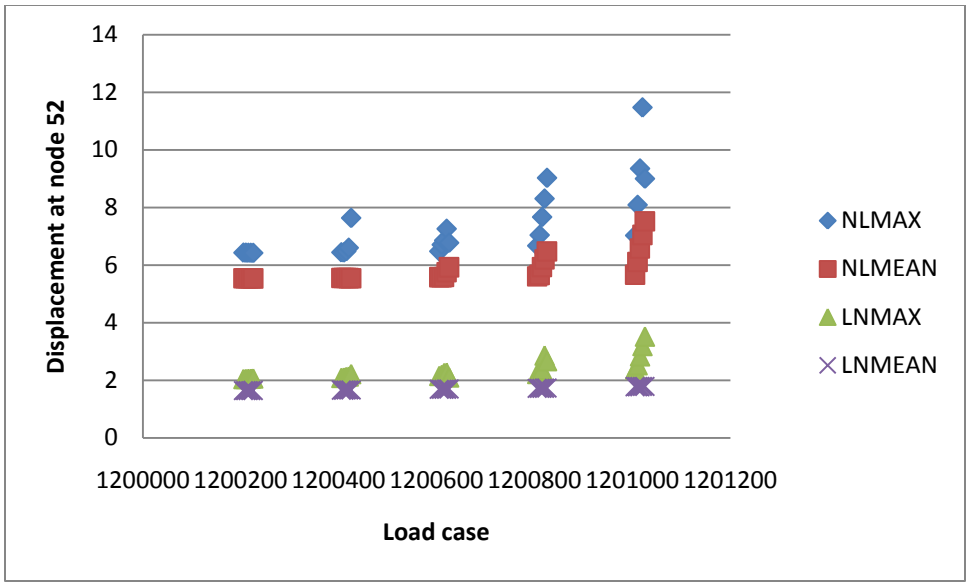

Figure 51 Trends of maximum and mean response of linear and nonlinear model for Mean wind speed of 120 mph

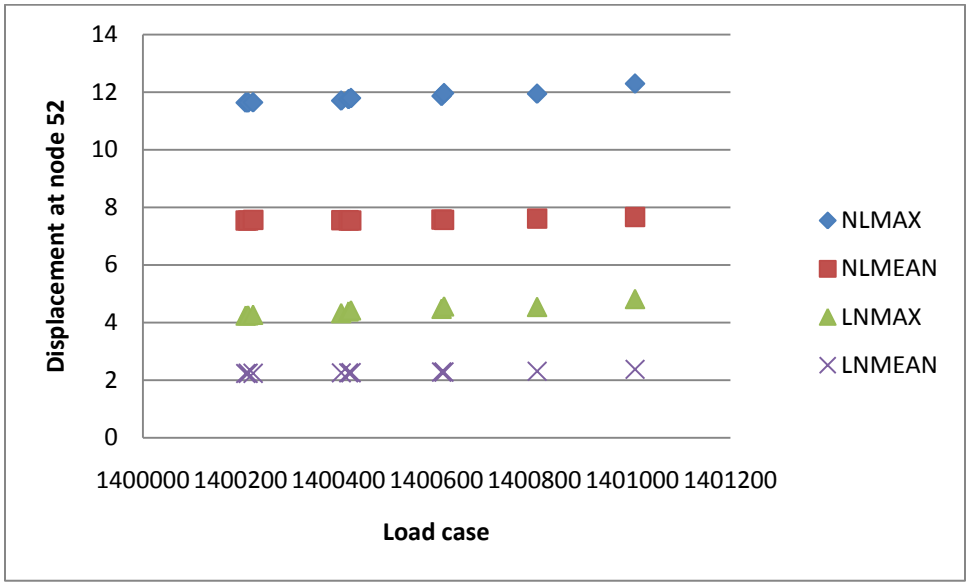

Figure 52 Trends of maximum and mean response of linear and nonlinear model for Mean wind speed of 140 mph

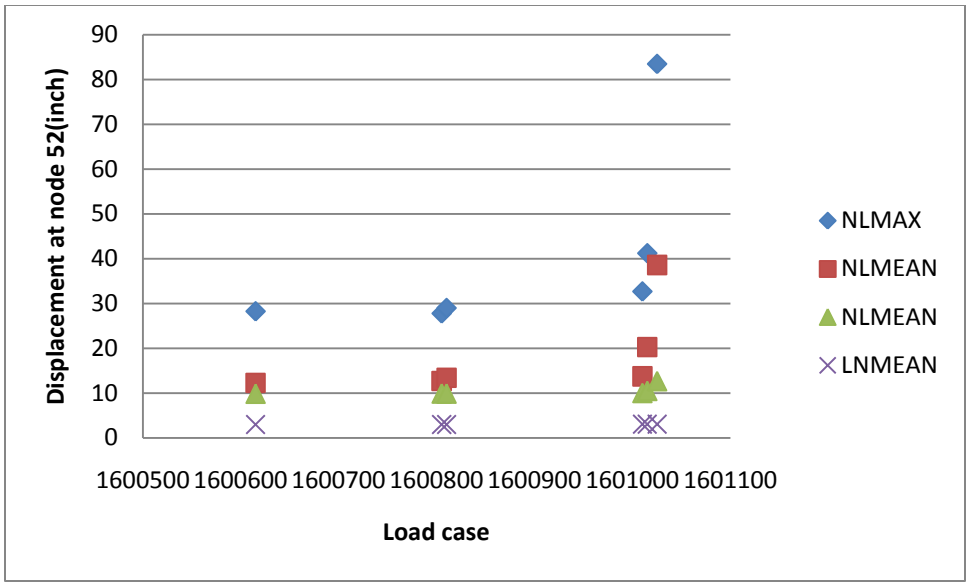

Figure 53 Trends of maximum and mean response of linear and nonlinear model for Mean wind speed of 160 mph

Table 8 Maximum and mean response of linear and nonlinear model for Mean wind speed of 80 mph

Case	NLMAX	NLMEAN	LNMAX	LNMEAN
800205	2.269	0.6872	2.462	0.7825
800210	2.267	0.6838	2.462	0.7302
800215	2.265	0.6854	2.461	0.731
800220	2.264	0.6877	2.46	0.732
800225	2.263	0.691	2.263	0.691
800405	2.278	0.7023	2.478	0.7474
800410	2.287	0.707	2.474	0.7478
800415	2.272	0.7147	2.479	0.749
800420	2.266	0.7229	2.55	0.7511
800425	2.32	0.7337	2.629	0.7454
800605	2.317	0.7373	2.503	0.7765
800610	2.309	0.7592	2.619	0.7767
800615	2.553	0.7687	2.708	0.778
800620	2.766	0.7792	2.954	0.7805
800625	2.999	0.7969	3.123	0.7845
800805	2.35	0.7792	2.588	0.8084
800810	2.645	0.8008	2.856	0.8081
800815	3.004	0.817	3.126	0.8091
800820	3.349	0.7602	3.416	0.8115
800825	3.729	0.9085	4.02	0.8155
801005	2.639	0.859	2.845	0.8695
801010	3.279	0.907	3.308	0.8683
801015	3.979	0.985	4.229	0.8689
801020	5.351	1.214	5.266	0.8713
801025	7.069	1.58	6.307	0.8759

Case	NLMAX	NLMEAN	LNMAX	LNMEAN
1000205	3.778	1.176	3.856896	1.201
1000210	3.773	1.177	3.851791	1.202
1000215	3.768	1.178	3.846687	1.203
1000220	3.763	1.18	3.841582	1.205
1000225	3.766	1.183	3.844645	1.208
1000405	3.783	1.197	3.862	1.157
1000410	3.797	1.2	3.859	1.157
1000415	3.81	1.204	3.856	1.159
1000420	3.817	1.211	3.853	1.161
1000425	3.857	1.22	3.889	1.164
1000605	3.835	1.233	3.888	1.186
1000610	3.854	1.243	3.88	1.186
1000615	4.061	1.26	4.406	1.187
1000620	4.301	1.283	4.214	1.19
1000625	4.517	1.312	4.383	1.194
1000805	3.892	1.275	3.916	1.128
1000810	4.179	1.3	4.116	1.218
1000815	4.537	1.34	4.386	1.219
1000820	4.962	1.401	4.659	1.221
1000825	5.63	1.509	4.93	1.225
1001005	4.184	1.365	4.105	1.127
1001010	4.841	1.44	4.568	1.278
1001015	5.947	1.616	5.035	1.278
1001020	7.224	1.775	5.554	1.289
1001025	8.218	2.084	6.649	1.29

Table 9 Maximum and mean response of linear and nonlinear model for Mean wind speed of 120 mph

Case	NLMAX	NLMEAN	LNMAX	LNMEAN
1200205	6.427	2.044	5.539	1.64
1200210	6.425	2.047	5.538	1.64
1200215	6.423	2.052	5.537	1.641
1200220	6.421	2.058	5.537	1.643
1200225	6.419	2.064	5.536	1.645
1200405	6.439	2.084	5.554	1.657
1200410	6.433	2.1	5.551	1.658
1200415	6.478	2.117	5.548	1.659
1200420	6.599	2.135	5.545	1.661
1200425	7.634	2.216	5.542	1.664
1200605	6.476	2.152	5.58	1.687
1200610	6.705	2.188	5.572	1.687
1200615	6.854	2.255	5.586	1.688
1200620	7.257	2.268	5.754	1.691
1200625	6.772	2.1	5.923	1.695
1200805	6.669	2.22	5.608	1.718
1200810	7.039	2.287	5.656	1.718
1200815	7.666	2.366	5.926	1.719
1200820	8.305	2.86	6.197	1.722
1200825	9.025	2.666	6.47	1.726
1201005	7.025	2.374	5.661	1.778
1201010	8.086	2.525	6.108	1.778
1201015	9.349	2.834	6.575	1.779
1201020	11.47	3.192	7.044	1.781
1201025	8.997	3.519	7.514	1.786

Table 10 Maximum and mean response of linear and nonlinear model for Mean wind speed of 140 mph

Case	NLMAX	NLMEAN	LNMAX	LNMEAN
1400205	9.485	3.596	7.539	2.231
1400210	11.63	4.238	7.538	2.232
1400215	11.63	4.245	7.537	2.233
1400220	9.562	3.609	7.537	2.234
1400225	11.64	4.265	7.563	2.236
1400405	9.592	3.64	7.554	2.249
1400410	11.7	4.323	7.551	2.249
1400415	10.96	4.02	7.548	2.251
1400420	11.75	4.383	7.545	2.253
1400425	11.79	4.42	7.542	2.256
1400605	9.016	3.706	7.58	2.278
1400610	11.86	4.472	7.572	2.278
1400615	11.96	4.557	7.565	2.28
1400620	11.97	3.713	7.574	2.282
1400625	12.35	3.705	7.743	2.286
1400805	11.94	4.538	7.608	2.31
1400810	8.892	3.76	7.596	2.31
1400815	12.36	3.756	7.745	2.311
1400820	4.962	1.404	8.106	2.313
1400825	5.63	1.505	8.29	2.317
1401005	12.29	4.813	7.661	2.371
1401010	11.14	3.835	7.928	2.37
1401015	10.99	3.963	8.395	2.37
1401020	10.98	4.665	8.791	2.374
1401025	12.59	4.007	10.34	2.382

*Censored data

Table 11 Maximum and mean response of linear and nonlinear model for Mean wind speed of 160 mph

Case	NLMAX	NLMEAN	LNMAX	LNMEAN
1600205	14.99	7.04	9.846	2.914
1600210	13.54	6.318	9.845	2.914
1600215	13.54	5.249	9.845	2.915
1600220	13.54	5.25	9.844	2.917
1600225	14.96	7.908	9.843	2.919
1600405	15.13	8.317	9.862	2.931
1600410	15.16	8.317	9.858	2.932
1600415	15.04	8.299	9.855	2.933
1600420	25.74	11.67	9.852	2.935
1600425	13.79	6.411	9.849	2.939
1600605	13.77	5.321	9.887	2.961
1600610	14.59	7.177	9.88	2.961
1600615	28.24	12.24	9.872	2.962
1600620	14.05	5.427	9.867	2.965
1600625	14.63	5.576	9.858	2.969
1600805	27.77	12.7	9.915	2.993
1600810	28.98	13.42	9.903	2.992
1600815	16.27	9.391	9.891	2.993
1600820	15.97	7.469	10.12	2.996
1600825	17.31	9.037	10.39	3
1601005	15	7.038	9.969	3.054
1601010	32.68	13.71	10.03	3.052
1601015	41.21	20.27	10.49	3.053
1601020	11.62	4.85	11.07	3.056
1601025	83.49	38.58	12.65	3.065

*Censored data

REFERENCES

ASCE. (2003). "Minimum design loads for buildings and other structures." *ASCE 7-02*, Structural Engineering Institute of the American Society of Civil Engineers, Reston, Va.

Atlantic Oceanographic and Meteorological Laboratory: The Saffir-Simpson Hurricane Scale http://www.nhc.noaa.gov/aboutsshs.shtml

Atlantic Oceanographic and Meteorological Laboratory (Ocean). (2005). HURDAT, http://www.aoml.noaa.gov/hrd/hurdat/easyhurdat_5107.html

Blake, E. S., Rappaport, E. N., Landsea C. W. The Deadliest, Costliest, and most intense United States Tropical Cyclones from 1851 to 2006 (and other frequently requested hurricane facts) NOAA Technical Memorandum NWS TPC-5

Batts M.E., Cordes M.R., Russell C.R., Shaver J.R. and Simiu E. (1980). *Hurricane wind speeds in the United States, National Bureau of Standards Report No. BSS-124*, US Department of Commerce, Washington, DC.

Coffman, B. F., Main, J. A., Duthinh, D. and Simiu, E. "Wind Effects on Low-Rise Buildings: Database-Assisted Design vs. ASCE 7-05 Standard Estimates," J. Struct. Eng. (in press).

Fernandes A. C., Henning J., Maia M. D., Sales J. S. (2008) Worst sea-Best sea group spectra from sea states

Georgiou P.N. (1985). Design wind speeds in tropical cyclone-prone regions, Ph.D. Dissertation, University of Western Ontario,.Russell L.R. (1971). Probability Distributions for Hurricane Effects. *ASCE J. Waterways Harbors Coastal Eng.***97** 1, pp. 139–154

Hawkes, P. J., Ewing, J. A., Harford, C. M., Klopman, G., Stansberg, C. T., Benoit, M., Briggs, M. J., Frigaard, P., Hiraishi, T., Miles, M., Santas, J., Schäffer, H. A. (1993). Comparative Analyses of Multidirectional Wave Basin Data, *Proceedings of the Second International Symposium OCEAN WAVE MEASUREMENT AND ANALYSIS*, Sponsored by the Waterways, Port, Coastal and Ocean Div., *ASCE*, 1993, New Orleans, Louisiana

Jelesnianski, C. P.,1967: Numerical computations of storm surges with bottom stress. *Mon. Wea. Rev*.,95, 770-756.

Jelesnianski, C. P., Chen, J. and W.A. Shaffer. (1992). SLOSH: Sea, Lake, and Overland Surges from Hurricanes. NOAA Technical Report NWS 48, United States Department of Commerce, NOAA, NWS, Silver Springs, MD., 71 pp

Krawinkler H. and Miranda E. (2004) “Performance-Based Earthquake Engineering”, *Earthquake Engineering from Engineering Seismology to Performance Based Engineering*, P 9/1-9/55

Main J. A. and Fritz W. A. (2006). "Database-Assisted Design for Wind: Concepts, Software, and Examples for Rigid and Flexible Buildings," *NIST Building Science Series 180*.

Neuman C. J., Jarvinen B.R., McAdie C.J. and Elms J.D. (1997). *Tropical cyclones of the North Atlantic Ocean, 1871–1996*, US Department of Commerce. Washington, DC.

Porter K. A. (2003) An Overview of PEER’s Performance Based Earthquake Engineering Methodology, *Ninth International Conference on Application of Statics and Probability in Civil engineering* (ICASP9), July 6-9, 2003, San Francisco.

Rosowsky, D., Sparks, P., and Huang, Z. (1999). “Wind field modeling and hurricane hazard analysis.” *Rep. to the South Carolina Sea Grant Consortium*, Dept. of Civil Engineering, Clemson Univ., Clemson, S.C.

Schroeder J. l., Smith D. A. (2003). Hurricane Bonnie wind flow characteristic as determined from WEMITE, *Journal of Wind Engineering and Industrial Aerodynamics* 91:767-789

Sheppard D. M., Miller W. (2003) “Design storm surge hydrographs for the Florida coast.” , Dept. of Civil and Coastal Engineering, University of Florida, FL

Simiu E. and Heckert H. (1996) Extreme wind distribution tails: a peaks over threshold approach. *Journal of .Structural. Engineering.. ASCE*122 5, pp. 539–547.

Simiu E. and Scanlan R. (1996). *Wind Effects on Structures* (3rd Edition ed.), Wiley, New York.

Structural Engineers Association of California(SEAOC). 1995. Vision 2000, Conceptual framework for performance based seismic design. *Recommended Lateral Force Requirements and Commentary* 1996, 6th edition sacramento CA:391-416

Vickery P.J. and Twisdale L.A. (1995). Wind-field and filling models for hurricane wind-speed prediction. *ASCE Journal of .Structural.Engineering.*121 11, pp. 1700–1

Vickery P.J., and L.A. Twisdale. (1995) Prediction of hurricane wind speeds in the United States. *ASCE Journal of .Structural .Engineering..*121 11, pp. 1691–1699.

Vickery, P. J., Skerlj, P. F., Steckley, A. C., and Twisdale, L. A. (2000a). “Hurricane wind field model for use in hurricane simulations.” *Journal of .Structural. Engineering..*, 126(10), 1203–1221.

Vickery, P. J., Skerlj, P. F., and Twisdale, L. A. (2000b). “Simulation of hurricane risk in the U.S. using empirical track model,” *Journal of .Structural .Engineering.*, 126(10), 1222–1237.

Wu C. S., taylor A. T.,Chen J., Shaffer W., (2003) “Tropical Cyclone Forcing of Ocean Waves”, conference on Costal Atmospheric and Oceanic Prediction and Processes Seattle, WA, 62-64

Yu B., Chowdhury A. G., Masters F. J., Hurricane. (2008). Wind Power Spectra, Cospectra and Integral Length Scales *Boundary Layer Meteorol*, 129:411-430